

# Generative Multi-purpose Sampler for Weighted M-estimation

Minsuk Shin

Department of Statistics, University of South Carolina,

Shijie Wang

Department of Statistics, University of South Carolina,

and

Jun S. Liu

Department of Statistics, Harvard University

## Abstract

To overcome computational bottlenecks of various data perturbation procedures such as the bootstrap and cross validations, we propose the *Generative Multi-purpose Sampler* (GMS), which directly constructs a generator function to produce solutions of weighted M-estimators from a set of given weights and tuning parameters. The GMS is implemented by a single optimization procedure without having to repeatedly evaluate the minimizers of weighted losses, and is thus capable of significantly reducing the computational time. We demonstrate that the GMS framework enables the implementation of various statistical procedures that would be unfeasible in a conventional framework, such as iteratedbootstrap procedures and cross-validation for penalized likelihood. To construct a computationally efficient generator function, we also propose a novel form of neural network called the *weight multiplicative multilayer perceptron* to achieve fast convergence. An R package called GMS is provided, which runs under `PyTorch` to implement the proposed methods and allows the user to provide a customized loss function to tailor to their own models of interest.

*Keywords:* Weighted M-estimation, Bootstrap/resampling, Cross-validation, Scalable Computation, Iterated Bootstrap

# 1 Introduction

Consider a canonical setting in which  $\mathbf{y} = \{y_1, \dots, y_n\}$  are i.i.d. observations following a statistical model with the parameter of interest denoted by  $\theta \in \Theta \subset \mathbb{R}^p$ . In some instances such as regression analysis, one may also include predictors or covariate variables for each observation. An efficient estimator of  $\theta$  can often be found by solving the following (penalized) optimization problem:  $\hat{\theta} = \operatorname{argmin}_{\theta} L_{\mathbf{y}}(\theta)$ , where  $L_{\mathbf{y}}(\theta) \equiv \frac{1}{n} \sum_{i=1}^n \ell_{\eta}(\theta; y_i)$  with  $\ell_{\eta}(\cdot)$  being a suitable loss function with an auxiliary parameter  $\eta$ . The resulting  $\hat{\theta}$  is often referred to as an *M-estimator* (Huber, 1992). For example, the maximum likelihood estimator (MLE) is a special M-estimator with the loss function being set as the negative log-likelihood function.

To assess the variability of the M-estimator  $\hat{\theta}$ , we study behaviors of the following tunable weighted M-estimators as inspired by the bootstrap methods (Efron, 1979):

$$\hat{\theta}_{\mathbf{w}, \lambda, \eta} = \operatorname{argmin}_{\theta} \left[ \frac{1}{n} \sum_{i=1}^n w_i \ell_{\eta}(\theta; y_i) + \lambda u(\theta) \right] \triangleq \operatorname{argmin}_{\theta} L_{\mathbf{y}}(\theta; \mathbf{w}, \lambda, \eta), \quad (1)$$

where  $\eta \in \mathbb{R}^+$  is an auxiliary parameter of the loss,  $u(\cdot)$  is a penalty function on the parameter with a tuning parameter  $\lambda$  that can be set to zero for non-penalized settings, and  $\mathbf{w} = (w_1, \dots, w_n)^{\top} \in \mathcal{W}$  is a vector of weights following distribution  $\pi(\mathbf{w})$ . The auxiliary parameter  $\eta$  tunes the loss function. For example, in quantile regression models,  $\eta \in (0, 1)$  represents the quantile level and the loss function takes the form  $\ell_{\eta}(\theta; y_i, X_i) = \rho_{\eta}(y_i - X_i^{\top} \theta)$ , where  $\rho_{\eta}(t) = t(\eta - I(t < 0))$ . When the loss function has no auxiliary parameter, we simply denote the loss and the resulting estimator by  $\ell(\theta; y_i)$  and  $\hat{\theta}_{\mathbf{w}, \lambda}$ , respectively.

The formulation of (1) applies to a wide range of statistical procedures. For example, the classical bootstrap procedure of Efron (1979) corresponds to  $\mathbf{w} \sim \text{Multinom}(n, \mathbb{1}_n/n)$ , where  $\mathbb{1}_n$  is a  $n$ -dimensional vector of one, and  $u(\theta) = 0$ . Random-weight bootstrap procedures can be formulated by imposing a general distribution on  $\mathbf{w}$  that has a mean of one, finite variance, and sum to  $n$ . Its theoretical properties such as consistency have been studied (Præstgaard and Wellner, 1993; Cheng and Huang, 2010; Barbe and Bertail, 2012). A special and most well-known form of the random-weight bootstrap is to set  $\mathbf{w} \sim n \times \text{Dirichlet}(n; \mathbb{1}_n)$  as in the *Bayesian Bootstrap* (Rubin, 1981) and *Weighted Likelihood Bootstrap* (Newton and Raftery, 1994). Theoretical

investigations and improvements of the bootstrap methods have been considered in a large body of literature (Chatterjee et al., 2005; McCarthy et al., 2018; Hall and Martin, 1988; Efron, 1987; Hahn, 1995; Kleiner et al., 2014).

Iterated bootstrap procedures are often employed to reduce the bias associated with a statistical inference procedure and/or improve the coverage precision of confidence intervals (Hall and Martin, 1988). A most frequently cited procedure is the double bootstrap, which first bootstraps and infers the parameter or prediction, and then estimates the bias of each bootstrapped solution via a second-level bootstrap. In (1), the double bootstrap procedures can be represented by setting a hierarchical weight distribution such that  $\mathbf{s} = \{s_1, \dots, s_n\} \sim \text{Multinom}(n, \mathbb{1}_n/n)$  and  $\mathbf{w} \mid \mathbf{s} \sim \text{Multinom}(n, \mathbf{s}/n)$ . These iterated bootstrap methods can be shown to provide more accurate confidence coverage (i.e., the second or higher-order accuracy) compared with single bootstraps and asymptotic approximations (Martin, 1992; McCarthy et al., 2018; Hall, 2013; Lee and Young, 1999, 1995). However, iterative bootstraps are computationally very expensive and are rarely used in practice when the data are of moderate to large sizes.

The tunable weighted M-estimation in (1) can also represent  $K$ -fold cross-validation. For pre-selected folds, such as a group of sample indices  $I_1, \dots, I_K$ , we set  $w_i = 0$  for  $i$  in the fold of interest, say  $I_1$ , and set  $w_i = 1$  in all other folds. This means that the observations in  $I_1$  will be ignored during training, rendering  $I_1$  to be test samples. If  $u(\cdot) = \|\cdot\|_1$ , the evaluated  $\hat{\theta}_{\mathbf{w}, \lambda}$  is equivalent to the LASSO estimator (Tibshirani, 1996), based on a tuning parameter  $\lambda$ , trained without using the samples in the considered fold  $I_1$ , resulting in a cross-validated LASSO. The computational burden of the cross-validation linearly increases with the fold size  $K$  and the candidate set size of the tuning parameter, and a typical amount is at least a few hundreds of repetitive computations.

While aforementioned weighted M-estimation procedures are widely used in statistics and science, the computational bottleneck caused by their repetitive nature poses significant practical difficulties. To alleviate these computational difficulties, we propose a computational strategy based on a neural network-based generative process, called the *Generative Multi-purpose Sampler* (GMS) (with the *Generative Bootstrap Sampler* (GBS) as a special case for bootstrap). Instead of repeating the same optimization process for various combinations of weights  $\mathbf{w}$ 's and

parameters  $\lambda$ 's and  $\eta$ 's, the GMS constructs a generator function that takes  $(\mathbf{w}, \lambda, \eta)$  as input and returns the corresponding weighted M-estimator  $\hat{\theta}_{\mathbf{w}, \lambda, \eta}$ . In addition to taking advantage of the high representation power of neural networks, a key idea for the GMS to achieve the desired computational efficiency gain is to minimize an integrative loss in the training of GMS, which optimizes both the M-estimation and the parameters employed by the GMS simultaneously.

The rest of the article is organized as follows. Section 2 introduces the general GMS framework and uses a toy example to explain its potential gains. Section 3 details its specialization for the bootstrap, namely the *generated bootstrap sampler* (GBS). Section 4 discusses the training of GMS for cross-validation with Lasso and quantile regression. Section 6 provides details on the neural network structures and detailed computational aspects of GMS. Section 7 concludes with a brief discussion.

## 2 Generative Multi-purpose Sampler

### 2.1 The basic formulation

We view the weighted M-estimator  $\hat{\theta}_{\mathbf{w}, \lambda, \eta}$  as a function of the weight  $\mathbf{w}$ , the tuning parameter  $\lambda$ , and the auxiliary parameter  $\eta$ , i.e.,  $G(\mathbf{w}, \lambda, \eta)$ , and attempt to approximate it by a member in a suitable family of functions  $\mathcal{G} = \{G_\phi : \mathbb{R}^{n+2} \mapsto \mathbb{R}^p, \phi \in \Phi\}$ , where  $\Phi$  is the space of parameters that characterize a function in the family. By doing so, we turn the unrestricted optimization problem in (1) into a restricted optimization problem in the functional space, i.e., finding a proper parameter of the generator function such that, for all  $\mathbf{w} \in \mathcal{W}$ ,  $\lambda \in \mathbb{R}^+$ , and  $\eta \in \mathbb{R}^+$ ,

$$\hat{\phi} = \operatorname{argmin}_{\phi \in \Phi} L_{\mathbf{y}}(G_\phi(\mathbf{w}, \lambda, \eta); \mathbf{w}, \lambda, \eta), \quad (2)$$

A slightly less ambitious, but more robust, formulation is to solve

$$\hat{\phi} = \operatorname{argmin}_{\phi \in \Phi} \mathbb{E}_{\mathbf{w}, \lambda, \eta} [L_{\mathbf{y}}(G_\phi(\mathbf{w}, \lambda, \eta); \mathbf{w}, \lambda, \eta)], \quad (3)$$

where  $\mathbb{E}_{\mathbf{w}, \lambda, \eta}(\cdot)$  is taken with respect to a proper distribution of  $(\mathbf{w}, \lambda, \eta)$  defined on  $\mathcal{W} \times \mathbb{R}^+ \times \mathbb{R}^+$ . We name this generative framework in (3) as the GMS. For non-penalized settings without the auxiliary parameter  $\eta$ , we simply denote the generator function by  $G(\mathbf{w})$ . We also use the notation  $\hat{G} = G_{\hat{\phi}}$ . The weight distribution for Efron's nonparametric bootstrap is simply  $\mathbf{w} \sim$

Multinom( $n, \mathbb{1}_n/n$ ). For the Bayesian bootstrap (Rubin, 1981),  $\mathbf{w}/n \sim \text{Dirichlet}(n, \mathbb{1}_n)$ . The distributions of  $\lambda$  and  $\eta$  can simply be the uniform distribution on candidate sets of  $\lambda$ 's and  $\eta$ 's chosen by the researcher. Another reasonable distribution of  $\lambda$  and  $\eta$  is to add random noises to a discrete set of candidate values (see Section 6.3 for details).

Suppose that  $\hat{\phi}$  is the solution of (3) for a sufficiently large family  $\mathcal{G}$  and a proper distribution on  $\{\mathbf{w}, \lambda, \eta\}$ ,  $\mathbb{P}_{\mathbf{w}, \lambda, \eta}$ , supported on  $\mathcal{W} \times \mathbb{R}^+ \times \mathbb{R}^+$ . If the solution  $\hat{\theta}_{\mathbf{w}, \lambda, \eta}$  of (1) is unique for any given  $(\mathbf{w}, \lambda, \eta)$  in the support, then  $G_{\hat{\phi}}(\mathbf{w}, \lambda, \eta)$  should be very close to  $\hat{\theta}_{\mathbf{w}, \lambda, \eta}$  almost surely in  $\mathbb{P}_{\mathbf{w}, \lambda, \eta}$ . It is easy to see this point by contradiction – if not, then there exist  $\epsilon > 0$  and a subset  $S^* \subset \mathcal{W} \times \mathbb{R}^+ \times \mathbb{R}^+$  such that  $\mathbb{P}_{\mathbf{w}, \lambda, \eta}(S^*) > 0$  and  $G_{\hat{\phi}}(\mathbf{w}, \lambda, \eta) \leq \hat{\theta}_{\mathbf{w}, \lambda, \eta} - \epsilon$  on  $S^*$ . Thus, we can find another function that differs from  $G_{\hat{\phi}}$  only on  $S^*$  and achieves a smaller value in (3).

A main takeaway from this argument is that optimizing the integrative loss over the space of  $(\mathbf{w}, \lambda, \eta)$  instead of the individual loss is appropriate for training. To benefit from this formulation, we must choose an appropriate family  $\mathcal{G}$  of functions  $G_{\phi}$  and a suitable distribution  $\mathbb{P}_{\mathbf{w}, \lambda, \eta}$  to cover the hyperparameter space of interest. As demonstrated by our empirical studies on a wide range of problems, restricting  $\mathcal{G}$  to be a class of neural networks and choosing a reasonable distribution  $\mathbb{P}_{\mathbf{w}, \lambda, \eta}$  appears to work well (see details in Section 6.3).

As shown in Cybenko (1989) and Lu et al. (2017), *Multi-Layer Perceptrons* (MLP), or equivalently, *Feed-forward Neural Networks* (FNNs), are theoretically capable of approximating any Lebesgue integrable function when the numbers of neurons and layers are sufficiently large. Also, recent successful applications of deep neural networks in a variety of data-rich fields provide compelling evidence supporting the use of over-parameterized MLPs and other types of neural networks for approximating extremely complicated functions (Goodfellow et al., 2014; Arjovsky et al., 2017). To train a neural network to achieve the task in (3), we employ a back-propagation algorithm (Rumelhart et al., 1986) along with *Stochastic Gradient Descent* (SGD) and its variants. More details are given in Section 6.1.

## 2.2 Intuitions for potential gains

Imagine that we have independent weight vectors  $(\mathbf{w}^{(1)}, \lambda^{(1)}, \eta^{(1)}), \dots, (\mathbf{w}^{(M)}, \lambda^{(M)}, \eta^{(M)})$  from  $\mathbb{P}_{\mathbf{w}, \lambda, \eta}$ , we can approximate the expectation in (3) by

$$\mathbb{E}_{\mathbf{w}, \lambda, \eta} [L_{\mathbf{y}}(G(\mathbf{w}, \lambda, \eta); \mathbf{w}, \lambda, \eta)] \approx \frac{1}{M} \sum_{m=1}^M L_{\mathbf{y}}(G(\mathbf{w}^{(m)}, \lambda^{(m)}); \mathbf{w}^{(m)}, \lambda^{(m)}, \eta^{(m)}). \quad (4)$$

$M$  do not need to be very large ( $M=100$ , say) since a small number of samples of  $(\mathbf{w}, \lambda, \eta)$  can be generated continuously within the iterative SGD algorithm to aid the fitting: after updating the FNN parameter  $\phi$  with SGD based on (4), we use the newly created samples to evaluate the fit and to provide refreshed gradient. Thus, the two optimization tasks, i.e., minimizing the loss function  $L_{\mathbf{y}}$  and finding optimal  $\phi$  for the generator  $G(\cdot)$ , co-evolve and help each other.

If we were to cast the task of training a generator in a classical machine learning framework, we would have to first obtain a set of training samples,  $\{(\mathbf{w}^{(b)}, \lambda^{(b)}, \hat{\theta}^{(b)})\}_{b=1}^B$ , where  $\hat{\theta}^{(b)} = \hat{\theta}_{\mathbf{w}^{(b)}, \lambda^{(b)}}$ , by evaluating  $B$  optimizations in (1) with  $(\mathbf{w}^{(b)}, \lambda^{(b)})$  for  $b = 1, \dots, B$  (ignoring  $\eta$  for simplicity in this case). Then, one may try to learn a function  $g$  by minimizing

$$\hat{g} = \operatorname{argmin}_g \sum_{b=1}^B \|\hat{\theta}^{(b)} - g(\mathbf{w}^{(b)}, \lambda^{(b)})\|^2, \quad (5)$$

under the  $l_2$ -distance  $\|\cdot\|$ . However, this squared-loss only measures the distance between the fitted generator  $\hat{g}(\mathbf{w}, \lambda)$  and its training true value  $\hat{\theta}_{\mathbf{w}, \lambda}$ . As a result, it cannot inform us how to improve the fitting of the original statistical loss in (1) other than a simple interpolation. Thus, the function trained in this manner tends to be inaccurate if  $B$  is small, or may be prohibitively expensive in computation if we must rely on a large  $B$ , in which case computational advantages of the generative process would be non-existing or limited.

Training the generator function  $G$  in conjunction with minimizing the loss function via the GMS formulation (3) is significantly more efficient. The classical loss (5) fits only on the training data with a limited size,  $\{(\mathbf{w}^{(b)}, \lambda^{(b)}, \hat{\theta}^{(b)})\}_{b=1}^B$ , resulting in an over-fitting issue. The GMS, on the other hand, is trained using the weights and tuning parameters generated from a predefined distribution without requiring additional optimizations for (1), and generating  $\mathbf{w}$  and  $\lambda$  is nearly cost-less. As a result, the GMS training procedure not only seeks the minimizer of  $L_{\mathbf{y}}(\theta; \mathbf{w}, \lambda)$ , but also allows for the use of an almost infinite number of training weights and tuning parameters during the training step, thereby avoiding over-fitting.

### 2.3 Illustration with a simple example

A novel aspect of our formulation is represented by the minimization of the integrative loss (3), which combines the individual optimization step required by each classical replication with the approximation of the functional form  $G$ . Let us consider the bootstrap procedure for a toy linear regression example with data  $(y_i, X_i)$ ,  $i = 1, \dots, n$ , and the loss function  $\ell(\theta; y_i, X_i) = (y_i - X_i^\top \theta)^2$  and  $\lambda = 0$ . For this problem, we can obtain the closed-form solution of the optimization problem for each bootstrapped sample:  $G_0(\mathbf{w}) = (\mathbf{X}^\top W \mathbf{X})^{-1} \mathbf{X}^\top W \mathbf{y}$ , where  $\mathbf{y} = (y_1, \dots, y_n)^\top$ ,  $\mathbf{X} = (X_1^\top, \dots, X_n^\top)^\top$ , and  $W = \text{diag}(\mathbf{w})$ . Thus, a bootstrap procedure would follow simple steps: for  $b = 1, \dots, B$ , generate  $\mathbf{w}^{(b)} = (w_1^{(b)}, \dots, w_n^{(b)}) \sim \text{Multinom}(n, \mathbb{1}_n/n)$  or  $n \times \text{Dirichlet}(n, \mathbb{1}_n)$ , and then for each  $\mathbf{w}^{(b)}$ , plug in the formula to get  $\hat{\theta}^{(b)} = G_0(\mathbf{w}^{(b)})$ . However, if one does not have the closed-form formula but has to solve numerically the minimization problem of (1) for every generated  $\mathbf{w}^{(b)}$ , the bootstrap procedure can be prohibitively demanding in computation. Thus, our GMS formulation via (3) can be thought of as an automatic way to find a highly accurate approximation to the closed-form solution (in the form of a neural network) of the minimization problem of (1). Once this solution  $\hat{G}$  is found, one can easily generate bootstrap estimators with almost no computational cost.

For a case of  $n = 100$  and  $p = 10$ , we set the true coefficient  $\theta = \{1, 0, \dots, 0\}$  and the regression variance one. The predictors are independently generated from  $N(0, I_p)$ . Even though this example is simple, constructing the generator function is non-trivial, because the generator function's domain dimension is 100, and the dimension of its codomain is 10. Training a 100-dimensional function with 10-dimensional codomain requires a large number of training samples in the framework of (5). This fact is reiterated in Figure 1. We generate a data set and evaluate random weight bootstrap estimators with  $\mathbf{w} \sim n \times \text{Dirichlet}(n; \mathbb{1}_n)$ , and then numerically evaluate the average loss of (1) on various weights from the trained generator for the classical machine learning approach with  $B = 500$  and  $B = 5,000$ , as well as the GMS. We initialize the optimization in different five points for each procedure.

We consider two performance measures for this example: the training loss specified in (5) and the *integrative prediction loss* (IPL) that can be defined as  $\mathbb{E}_{\mathbf{w}} \|\hat{\theta}_{\mathbf{w}} - g(\mathbf{w})\|^2$ . The IPL is approximated by using 1,000,000 Monte Carlo evaluations, and the loss values are multiplied by

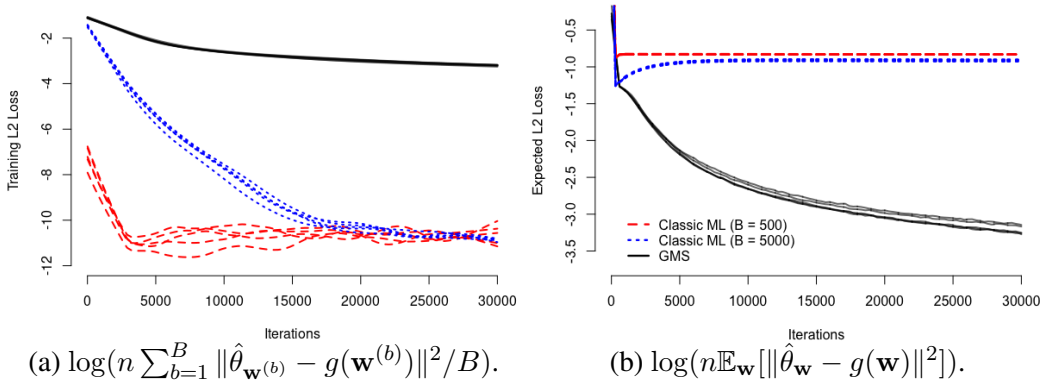


Figure 1: Trace plots of (a) the training loss, and (b) the integrative prediction loss, in the logarithmic scale. Five lines for each optimization represent five distinct initializations; and the red dashed and blue dotted lines indicate the conventional ML with  $B = 500$  and  $B = 5000$ , respectively.

$n$  to adjust for the scale of  $\text{Var}(\hat{\theta})$ . Note that the GMS trains its generator  $G$  by minimizing the integrative loss (3), whereas the naive generator  $g$  is trained using the  $l_2$ -loss in (5) with  $B = 500$  and 5,000 training samples, respectively. As expected, Figure 1(a) shows that the training  $l_2$ -losses for the naive procedures are significantly lower than those for the GMS. However, the IPLs of the considered methods behave quite differently. The naive minimizers (for the cases with  $B = 500$  and 5,000) first decrease their IPLs rapidly, but after 200 iterations their IPLs begin to increase. In contrast, the GMS seamlessly reduces its IPL. The poor predictive performance of the naive procedure stems from the fact that the  $l_2$ -loss encourages the generator function  $\hat{g}$  to overfit the training set  $\hat{\theta}^{(1)}, \dots, \hat{\theta}^{(B)}$ . Unlike the conventional machine learning modeling, the GMS is quite resistant to overfitting, as we can sample  $\mathbf{w}$ 's at near-zero computational cost during the training of the generator function.

### 3 Generative Bootstrap Samplers

#### 3.1 Bootstrap and subgroup bootstrap

The simplest use of the GMS is to bootstrap M-estimators, which is a special case of form (3) without  $\eta$  and  $u(\cdot)$ . The weight distribution is  $\text{Multinom}(n, \mathbb{1}_n/n)$  (or  $n \times \text{Dirichlet}(n, \mathbb{1}_n)$  for the Bayesian bootstrap). More precisely, we let  $\phi$  be the parameter underlying the generator  $G$  and solve the optimization problem:  $\hat{\phi} = \text{argmin}_{\phi \in \Phi} \mathbb{E}_{\mathbf{w}} [\frac{1}{n} \sum_{i=1}^n w_i \ell(G_{\phi}(\mathbf{w}); y_i)]$ . We call this simple GMS application the *Generative Bootstrap Sampler* (GBS).

Despite its considerable efficiency, the GBS framework has a fundamental limitation for prac-



tical bootstrap applications: the dimension of the generator domain equals the sample size  $n$ . Even when computationally efficient neural networks are used to model the generator, the convergence is quite slow when the input dimension is high (say, tens of thousands). We may further encounter technical issues such as memory shortage as well, which is particularly severe for big data. To address this limitation, we consider a subgroup weighting strategy, which divides the data set into subgroups and assigns equal weights to observations within each subgroup. The subgrouping idea is primarily used for bootstrapping time series data sets, referred to as *block bootstrap* (Lahiri, 1999; Härdle et al., 2003), in order to preserve the temporal association within bootstrapped samples. In contrast to the time series applications, we use subgrouping (or blocking) to reduce the number of weights, or more precisely, the domain dimension of the generator function so as to save computational costs.

Let  $[n]$  denote the index set  $\{1, \dots, n\}$  of the observations. We consider an exclusive and exhaustive partition:  $I_1, \dots, I_S \subset [n]$  such that  $I_i \cap I_j = \emptyset, \forall i \neq j$ , and  $\cup_{s=1}^S I_s = [n]$ . Without loss of generality, we assume that the size of each  $I_s$  is the same, i.e.,  $|I_s| = n/S$  for  $s = 1, \dots, S$ . We define a subgroup assignment function  $h : [n] \mapsto [S]$  such that  $h(i) = s$  if  $i \in I_s$ . Then, for  $\{\alpha_1, \dots, \alpha_S\}^T \sim \mathbb{P}_\alpha$ , with  $\mathbb{P}_\alpha$  being an  $S$ -dimensional weight distribution, we impose the same value of weight on all elements in a subgroup as

$$w_i = \alpha_{h(i)} \quad \text{for } i = 1, \dots, n. \quad (6)$$

and we denote  $\mathbf{w}_\alpha = \{\alpha_{h(1)}, \dots, \alpha_{h(n)}\}^T \in \mathbb{R}^n$ . As a result, it follows that  $\alpha_{h(i)} = \alpha_{h(k)}$ , if  $i, k \in I_s$  for some  $s$ . Similar to the vanilla GBS, setting  $\alpha \sim \text{Multinomial}(S, \mathbb{1}_S/S)$  or  $\alpha \sim S \times \text{Dirichlet}(S, \mathbb{1}_S)$  result in the block-based nonparametric bootstrap and Bayesian bootstrap, respectively.

As an illustration, we consider a simple linear regression example by generating a data set from the model with  $n = 1000, p = 10$ , the coefficients being a sequence of equi-spaced values between  $-2$  and  $2$ , and  $\sigma^2 = 2$ . Each covariate is drawn i.i.d. from  $N(0, 1)$ , and the regression variance is set to one. The resulting domain dimension of a vanilla  $G$  is 1000. Figure 2 shows individual histograms of bootstrap distributions with varying subgroup sizes. Even when the number of subgroups is tiny ( $S = 5$ ), the obtained bootstrap distributions are acceptable, although the variability tends to be underestimated. As  $S$  increases ( $S = 25$ ), the quality of the

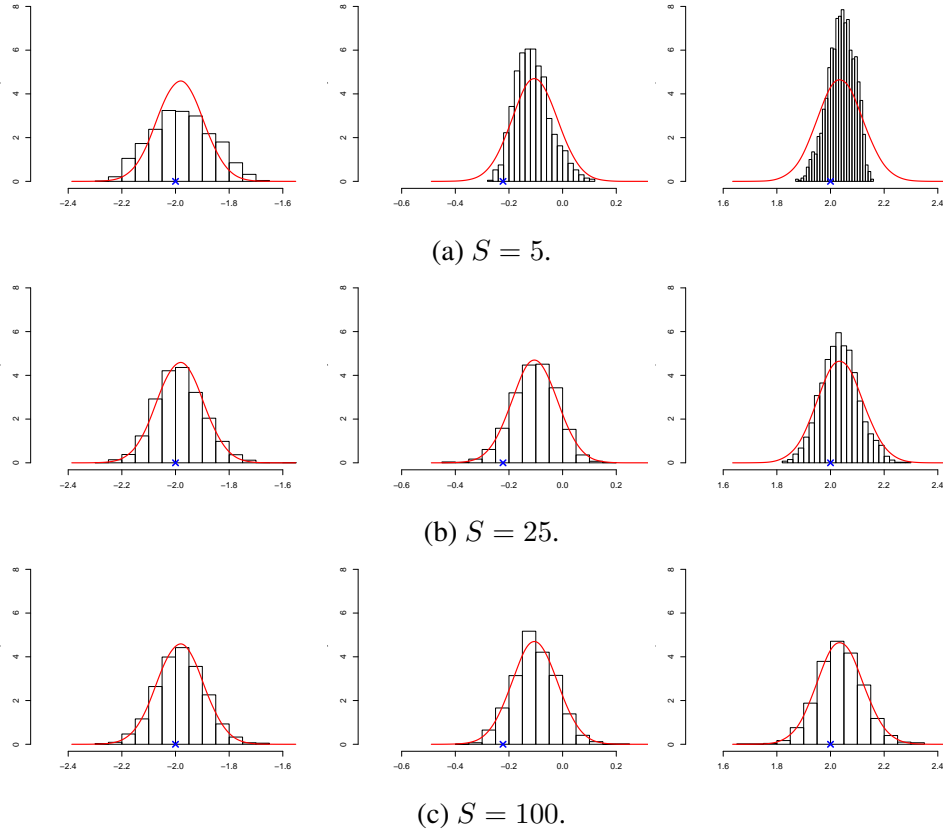


Figure 2: Histograms of block bootstrap distributions with various  $S$  for the coefficient of  $X_1$  (top),  $X_5$  (middle), and  $X_{10}$  (bottom) for each subfigure. The red line indicates the density function of the target distribution (of the standard bootstrap).

approximation of the subgroup bootstrap distribution improves significantly. When  $S = 100$ , the subgroup bootstrap distributions are indistinguishable from the target ones. When we use 100 subgroups (10 observations in each subgroup), the input dimension is reduced to 100 from the original 1000 but the resulting bootstrap distributions are nearly identical to those from the standard bootstrap (see Figure 3).

**Remark.** Under some regularity conditions, one can show that the subgroup bootstrap is consistent when  $S$  is of a higher order than  $\sqrt{n}$  (see the Supplementary Materials for a formal proof).

### 3.2 Iterated bootstrap

The iterated bootstrap method was proposed to improve the inference accuracy of the simple bootstrap method, and was shown both theoretically and empirically to achieve a higher-order

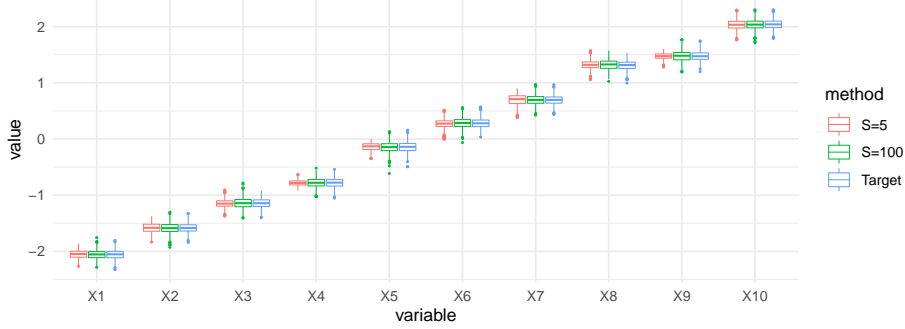


Figure 3: Comparisons of subgroup bootstraps across different numbers of blocks.

accuracy for the coverage of the constructed confidence intervals and bias-corrections (Martin, 1992; McCarthy et al., 2018; Hall, 2013; Lee and Young, 1999, 1995). More precisely, an iterated bootstrap procedure involves nested levels of data resampling.

The double bootstrap, which is the simplest iterated bootstrap, first creates  $B$  bootstrap samples,  $\mathbf{y}_b^*$ , for  $b = 1, \dots, B$  by resampling from the original data set, and then, for each bootstrapped sample  $\mathbf{y}_b^*$ , creates  $C$  second-level bootstrap samples,  $\mathbf{y}_{bc}^{**}$ ,  $c = 1, \dots, C$ , by resampling from  $\mathbf{y}_b^*$ . For each  $\mathbf{y}_b^*$  and  $\mathbf{y}_{bc}^{**}$ , we denote the corresponding estimator of  $\theta$  by  $\hat{\theta}_b^*$  and  $\hat{\theta}_{bc}^{**}$ , respectively. By iterating this step, we can simply extend this to more iterated bootstrap cases.

Various procedures for constructing confidence intervals using bootstrap have been proposed, such as the *percentile* method (Hall, 1992), the *studentized* method (Hall, 1988; Efron, 1979), the *Bias-Corrected and accelerated* method  $BC_a$  (Efron, 1987), and *Approximated Bias Correction* (ABC; Dicciccio and Efron (1992)), etc. Even though  $BC_a$  and ABC procedures enjoy the second-order accuracy (fast convergence in coverage error), a practical implementation of these procedures are not trivial since it is difficult to calculate their acceleration factor for general models. On the other hand, the percentile procedure is only first-order correct, and the studentized procedure requires an iterated bootstrap unless an explicit form of the standard error of the bootstrap estimator is available. To improve the quality of the constructed CI, we consider using double bootstraps as in the coverage calibration method (Hall and Martin, 1988; Hall, 1986) and studentized CI procedure (Hall, 1988). The calibrated percentile two-sided CI via double bootstrap achieves the second-order accuracy  $O(n^{-1})$ , while its single bootstrap counterpart only attains a rate of  $O(n^{-1/2})$ . However, applying the conventional double bootstrap requires undesirably intensive computation: a total of  $B \times C$  evaluations of bootstrap estimators  $\hat{\theta}_{bc}^{**}$  for

$b = 1, \dots, B$  and  $c = 1, \dots, C$ . Lee and Young (1999) showed that  $B$  and  $C$  should be of a higher order than  $n^4$  and  $n^2$  for two-sided CIs and of order  $n^2$  and  $n$  for one-sided CIs, respectively, so that the coverage error rate of the Monte Carlo interval is no greater than that of the theoretical double bootstrap interval. The authors considered  $B = 1000$  and  $C = 500$  in their simulations, resulting in a total of 500,000 evaluations, which is an unmanageable size under the conventional bootstrap framework.

### 3.3 GBS for iterated bootstrap

Extending the GBS to iterated bootstraps is immediate as it is a special case of (3) with a weight distribution that has a hierarchical structure. For a  $d$ -level iterated bootstrap procedure, we may characterize its weight distribution hierarchically:  $\mathbf{w}_{(1)} \sim \text{Multinom}(n, \mathbb{1}_n/n)$ ,  $\dots$ ,  $\mathbf{w}_{(d)} \mid \mathbf{w}_{(d-1)} \sim \text{Multinom}(n, \mathbf{w}_{(d-1)}/n)$ . The computational advantage of the GBS framework is particularly significant in these iterated situations.

One drawback of the standard nonparametric bootstrap is that each bootstrap sample only touches upon about  $1 - e^{-1} \approx 63\%$  of the observations due to the nature of multinomial sampling, which appears to be somewhat wasteful. This loss is compounded and become more significant in iterated bootstraps. A smoothed version of these weight distributions is a hierarchy of Dirichlet distributions, which enable each  $\hat{\theta}_b^*$  and  $\hat{\theta}_{bc}^*$  to utilize all the observations (Cheng and Huang, 2010; Xu et al., 2020; Præstgaard and Wellner, 1993). Thus, we mainly consider  $\mathbf{w} \mid \mathbf{z} \sim n \times \text{Dirichlet}(n, \mathbf{z})$  and  $\mathbf{z} \sim n \times \text{Dirichlet}(n, \mathbb{1}_n)$ . If a subgroup bootstrap as in Section 3.1 is employed the subgrouped weights follow  $\mathbf{w} \mid \mathbf{z} \sim S \times \text{Dirichlet}(S, \mathbf{z})$  and  $\mathbf{z} \sim S \times \text{Dirichlet}(S, \mathbb{1}_S)$ . We train a generator function that covers both single and double bootstraps by adopting a probabilistic mixture of single and double bootstrap weights distributions; e.g., generate single or double bootstrap weights with 50%-50% chances.

### 3.4 An illustration: double-bootstrap for logistic regression

We consider the standard logistic regression model:  $y_i \sim \text{Bernoulli}\left(\frac{1}{1 + \exp\{-X_i^T \theta\}}\right)$ , where  $X_i \in \mathbb{R}^p$  and  $\theta \in \mathbb{R}^p$  for  $i = 1, \dots, n$ . To apply the GBS to this model, we simply set  $\ell(\theta; y_i) = (1 - y_i) \log X_i^T \theta + \log(1 + \exp(-X_i^T \theta))$  in (3). We simulate a data set that contains  $n = 400$

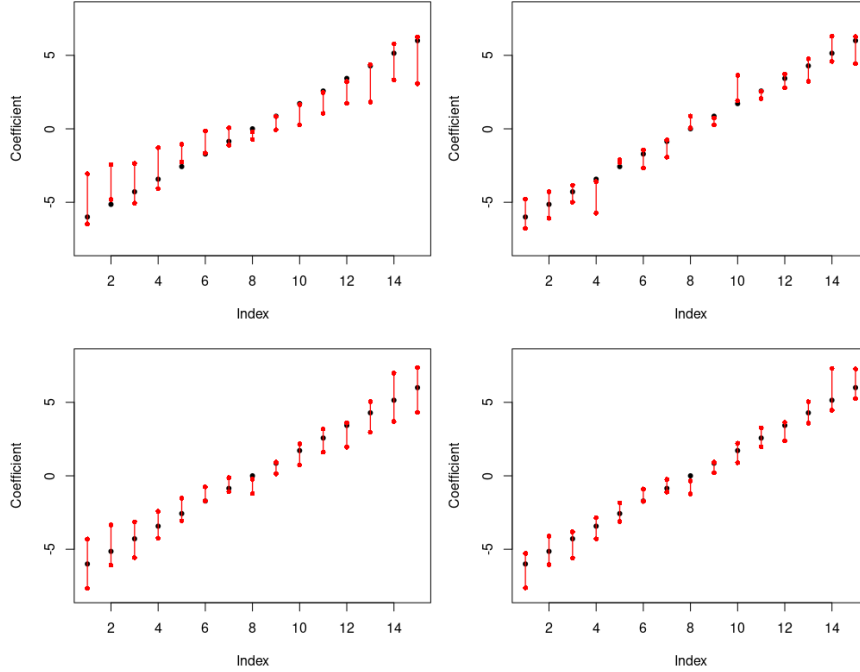


Figure 4: 95% CIs for the logistic regression example: The basic single bootstrap CI (top left); the BCa CI (top right); the calibrated percentile bootstrap CI via double bootstrap (bottom left); a studentized bootstrap CI via double bootstrap (bottom right). True parameters are marked by black dots.

observations, each with  $p = 20$  covariates generated independently from the standard Gaussian. The true coefficient vector is set to be an equi-spaced sequence between  $-6$  and  $6$ .

We examine 95% CIs constructed by various procedures, including a bias-corrected percentile CI (single bootstrap, denoted by “basic”), a BCa CI (Efron, 1987), a calibrated percentile CI (double bootstrap), and a studentized CI (double bootstrap). The “basic” CI is constructed as  $(2\hat{\theta} - q_{97.5\%}^*, 2\hat{\theta} - q_{2.5\%}^*)$ , where  $q_{\beta}^*$  is the  $\beta$ -quantile of the bootstrap distribution of  $\hat{\theta}^*$ . The calibrated percentile CI is obtained as  $(2\hat{\theta} - q_{\hat{\alpha}_U}^*, 2\hat{\theta} - q_{\hat{\alpha}_L}^*)$ , where  $\hat{\alpha}_L$  and  $\hat{\alpha}_U$  are calibrated coverage levels via the double bootstrap aiming at 2.5% and 97.5%, respectively. The studentized CI is  $(\hat{\theta} - \tilde{t}_{97.5\%}^* \hat{s}, \hat{\theta} - \tilde{t}_{2.5\%}^* \hat{s})$ , where  $\tilde{t}_{\beta}^*$  is the  $\beta$ -quantile of the studentized bootstrap statistic, and  $\hat{s}$  is the estimated standard error (a detailed description of these bootstrap procedures is given in Section B of the supplementary materials). Figure 4 shows that, despite the fact that the single bootstrapped CI (top left) is bias-corrected, the resulting CI is strongly biased and its width is excessively wide with a low coverage (12/20), and BCa suffers from a similar issue. In contrast, the two double bootstrap procedures result in better CIs by both shortening the widths and

improving the coverage accuracy (19/20 coverage for both the calibrated and the studentized).

For the double bootstrapped CIs, we generate 5000 bootstrap samples for the first-level and 1000 for the second-level, resulting in a total of  $5000 \times 1000 = 5,000,000$  bootstrap evaluations. This poses a significant computational challenge under the conventional framework. In comparison, once the generator function is trained (which takes less than 3 minutes for this example), the GBS produces 10,000 bootstrap estimators in less than 0.1 second, and its computational advantage is even more significant when  $n$  and  $p$  are larger, as shown next.

### 3.5 Scaling up towards large $n$ and $p$

We consider the same logistic regression model as in Section 3.4 with the true regression coefficients  $\theta_j$ 's equally spaced between  $-3$  and  $3$ . We compare the performance of the GBS with those of the standard bootstrap, BCa, and the profile likelihood confidence interval with sample size  $n \in \{500, 5000, 10000\}$  and dimension of covariates  $p \in \{30, 200, 300\}$ . This simulation is replicated independently 20 times. We examine properties of the 95% CIs constructed by these bootstrap methods (i.e., the average coverage and average width, and their actual computing time). For standard bootstrap procedures, we consider both a parallel computing environment using 25 CPU cores (abbreviated as “25C”), and a single-core computation (i.e., “1C”). The detailed setting is described in Section 6.3, and the specification of the computing server is given in the the supplementary materials. We use the R package `boot` to implement conventional bootstrap procedures. The profile likelihood CI is based on an asymptotic approximation, and its computation is carried out by using the `confint` function in R. Due to the computational burden, the conventional CI procedures for large sized data sets are too expensive, so we only report the estimated computation times using two replicates.

Table 1 compares traditional bootstrap procedures with their GBS equivalents in various settings. The GBS procedures are comparable to their conventional counterparts (“Basic” and “Percentile” in the table) in terms of the coverage and width of the constructed CIs. When  $(n, p) = (500, 30)$ , the traditional bootstrap-based CIs are significantly faster to compute. However, as data size increases, the conventional bootstrap becomes prohibitively expensive, taking more than an hour for  $(n, p) = (10000, 300)$  using a parallel computation with 25C, and more

Method	$(n, p) = (500, 30)$			$(n, p) = (5000, 200)$			$(n, p) = (10000, 300)$		
	Cov	Width	Time	Cov	Width	Time	Cov	Width	Time
GBS1 (Basic)	0.975	1.804	140.8 + 0.1	0.987	1.028	152.9 + 0.2	0.976	0.721	163.6 + 0.4
GBS1 (Percentile)	0.752	1.804	140.8 + 0.1	0.217	1.028	152.9 + 0.2	0.199	0.721	163.6 + 0.4
GBS2 (Student)	0.962	1.548	140.8 + 15.6	0.960	0.904	152.9 + 45.0	0.931	0.651	163.6 + 63.9
GBS2 (Calibrated)	0.933	1.463	140.8 + 15.6	0.954	0.894	152.9 + 45.0	0.938	0.661	163.6 + 63.9
Basic (25C)	1.000	1.899	8.4	1.000	1.237	539.6	NA	NA	4227.05
Basic (1C)			93.8			3833.3			25540.5
Percentile (25C)	0.760	1.899	8.4	0.230	1.237	539.6	NA	NA	4227.05
BCa (25C)	1.000	2.039	84.3	NA	NA	NA	NA	NA	NA
Profile	0.918	1.657	0.7	0.462	0.941	1310.8	NA	NA	8670.7

Table 1: Results of the simulation study for logistic regression models; “GBS1” and “GBS2” indicate single and double bootstraps implemented by the GBS, respectively; “Cov”, “Width”, and “Time” mean the averages (over 20 replicates) of the coverage, the width, and the actual computing time (seconds) of each evaluated 95% CI, respectively; for the computation time of the GBS, the black and red numbers indicate training and generation time (including post processing time for the GBS), respectively.

than 7 hours using 1C. Due to its heavy computational need, the BCa cannot produce meaningful results for moderately large data sets (e.g., for  $(n, p) = (5000, 200)$  and  $(10000, 300)$ ). The profile likelihood procedure (“Profile”), which is based on an asymptotic approximation of the sampling distribution, is also quite expensive when data size becomes large.

For the double bootstraps, the conventional repetitive computations take more than 2.5 hours with parallel computation using 25C for the case with  $(n, p) = (500, 30)$ , and would have taken more than 48 days for the case with  $(n, p) = (10000, 300)$ . As a result, the conventional double bootstrap procedures are infeasible for multiple replicates, so their results are omitted in Table 1. In contrast, the GBS training takes less than three minutes for all examined settings, while the generation and post-processing for the double bootstrap take about one minute. Furthermore, the double-bootstrap GBS2s requires very little extra computational time, but achieves a significantly higher accuracy, than the single bootstrap GBS1s.

## 4 Bootstrap Cross-Validation for Parameter Tuning Via GMS

Tuning parameter selection has been a challenging and computationally intensive task for many statistical and machine learning algorithms since repetitive computations are often required over a wide range of possible choices of the tuning parameter. We note that the GMS framework is not only applicable to bootstrap, but can also be used to expedite the computation of *Cross-*

*Validation (CV)* procedures. It is easy to see that for a weight  $w_i = 0$ , the corresponding term in the weighted M-estimation loss function (1) is zero, which is equivalent to ignoring observation  $y_i$ . More generally, we denote  $\mathbf{w}_{(-I)} = \{w_1, \dots, w_n\}$  with  $w_i = 0$  for  $i \in I$ , and  $\{w_i : i \notin I\} \sim (n - |I|) \times \text{Dirichlet}(n - |I|; \mathbb{1}_{n-|I|})$ . Thus, index sets  $I$  and  $I^c$  can be viewed as those for the test and training data, respectively. To train the CV generator without the bootstrapping aspect, one may employ a simpler weight distribution than the multinomial or Dirichlet, such as setting all the weights in a randomly selected fold to be zero, and the remaining to be one. Based on this setup, a simple modification of Algorithm 1 (with strategies in Section 6.3) can be used to train the generator for the  $K$ -fold CV (more details in the Supplementary Materials). Once the generator is trained, one can easily compute the estimated out-of-sample error across different tuning parameters by alternating zero weight for each fold.

More precisely, for  $b = 1, \dots, B$  and a tuning parameter  $\lambda_l$  in a candidate set  $\{\lambda_1, \dots, \lambda_L\}$ , we set zero weights on a fold  $I_k^*$  for  $k = 1, \dots, K$ ; i.e.,  $w_i^{(b,k)} = 0$  for  $i \in I_k^*$ . For  $i \notin I_k^*$ , we can set  $w_i^{(b,k)} = 1$  when only CV is of interest, or let  $\{w_i^{(b,k)}\}_{i \notin I_k^*} \sim (n - |I_k^*|) \times \text{Dirichlet}(n - |I_k^*|, \mathbb{1}_{n-|I_k^*|})$  so as to quantify uncertainty in the CV via bootstrap. The bootstrapped CV estimator without considering the test set  $I_k^*$  with a tuning parameter  $\lambda_l$ , denoted by  $\hat{\theta}_{(-I_k^*), \lambda_l}^{(b)}$ , can be computed as  $\widehat{G}(\mathbf{w}^{(b,k)}, \lambda_l)$ . The CV loss for the  $k$ -th fold and  $\lambda_l$  follows as  $\hat{e}_l^{(b,k)} = \sum_{i \in I_k^*} \ell(\hat{\theta}_{(-I_k^*), \lambda_l}^{(b)}; y_i) / |I_k^*|$ . After repeating this step for all the  $K$  folds, we obtain the bootstrapped  $K$ -fold CV errors as  $\bar{e}_l^{(b)} = \sum_{k=1}^K \hat{e}_l^{(b,k)} / K$ . After obtaining  $\bar{e}_l^{(b)}$  for  $l = 1, \dots, L$  and  $b = 1, \dots, B$ , one can easily identify the bootstrap distribution of the out-of-sample loss via the empirical distribution of  $\{\bar{e}_l^{(b)}\}_{b=1, \dots, B}$  under  $\lambda_l$ , as well as confidence bands of the out-of-sample loss over  $\{\lambda_1, \dots, \lambda_L\}$ .

Moreover, with  $l^{(b)} = \text{argmin}_l \{\bar{e}_l^{(b)}\}$ , the empirical distribution of  $\{\lambda_{\min}^{(b)} \triangleq \lambda_{l^{(b)}}\}$ ,  $b = 1, \dots, B$  serves as the bootstrap distribution of the minimizer of CV errors and can naturally quantify the uncertainty of the chosen tuning parameter (an example is given in the left of Figure 6). For example, this bootstrap distribution  $\{\lambda_{\min}^{(b)}\}$  provides us an alternative to the *ad hoc* one-standard-error rule commonly recommended for Lasso regression, in which one chooses the most parsimonious model whose CV error is no more than one standard deviate above that of the best model. In contrast, with the availability of the bootstrap distribution of  $\lambda_{\min}$ , we may pursue



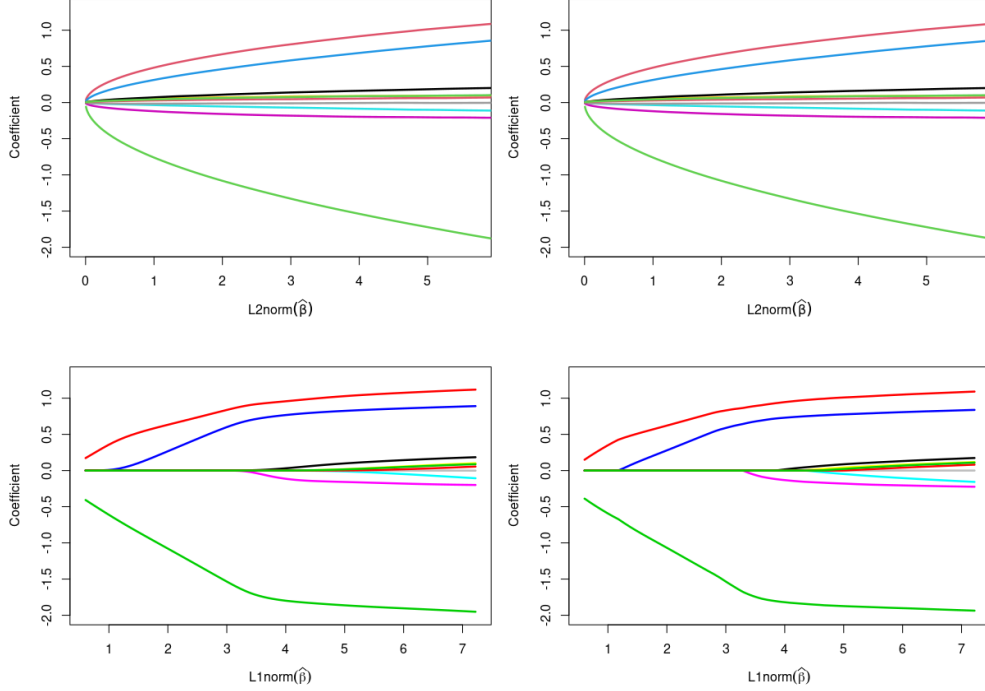


Figure 5: Solution paths of the GMS ridge (top left), the standard ridge regression (top right) and the GMS LASSO (bottom left), and the LARS (bottom right).

a more parsimonious model by using the lower  $(1 - \alpha)\%$  confidence bound of this distribution as our chosen  $\lambda$ .

**Cross-validation for LASSO and ridge regression.** Two representative examples of the penalized M-estimation are ridge (Hoerl and Kennard, 1970) and LASSO regression models (Tibshirani, 1996), with the corresponding loss function for GMS:

$$\mathbb{E}_{\mathbf{w}, \lambda} \left[ \frac{1}{n} \sum_{i=1}^n w_i \{y_i - X_i^T G(\mathbf{w}, \lambda)\}^2 + \lambda u(G(\mathbf{w}, \lambda)) \right], \quad (7)$$

with  $u(x) = \|x\|_2^2$  for the ridge regression and  $u(x) = \|x\|_1$  for the LASSO. After obtaining the trained  $\hat{G}$  from (7), for a given input  $\mathbf{w}^*$  and  $\lambda^*$ , its output  $\hat{G}(\mathbf{w}^*, \lambda^*)$  approximates the minimizer of  $\sum_{i=1}^n w_i^* \ell(\theta; y_i) / n + \lambda^* u(\theta)$  with respect to  $\theta$ . We simulated from a linear regression model with  $n = 500$ ,  $p = 50$ , the true parameter  $\theta_0 = \{1, -2, 1, 0, \dots, 0\}$ , and  $\sigma_0^2 = 1$ . Each covariate vector  $X_i$  follows iid  $N(0, \Sigma)$  with  $\Sigma_{kl} = 1$  for  $k = l$  and  $\Sigma_{kl} = 1/2$  for  $k \neq l$ .

Figure 5 shows solution-path plots that depict the relations between the tuning parameter

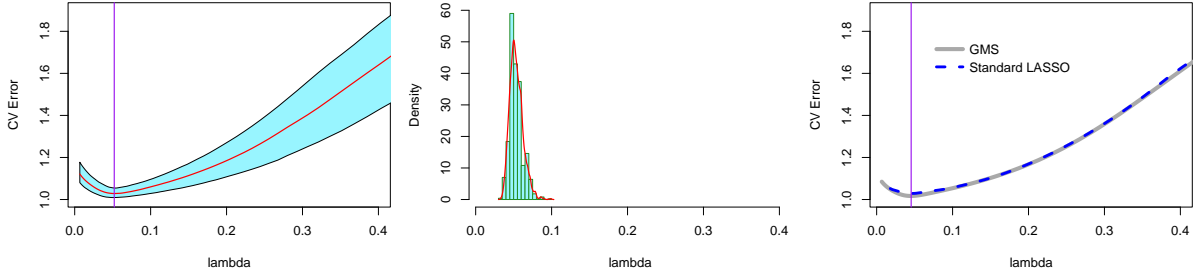


Figure 6: Left: The 95% confidence band of CV error evaluated from the GMS bootstrap with random weights, and the red solid line indicates the mean curve. Middle: The GMS bootstrapped distribution of the CV-error minimizer  $\lambda_{\min}$ . Right: CV errors based on the standard LASSO and the GMS with the constant weight vector  $\mathbb{1}$ . The purple vertical line indicates the value of  $\lambda$  that minimizes the CV error.

choices and the corresponding estimated ridge and LASSO estimators. The  $x$ -axis indicates the  $l_2$  norm of the ridge regression or  $l_1$  norm of the LASSO estimators based on a series of  $\lambda$ 's, and the  $y$ -axis, the value of the estimated coefficient. After the generator is trained by minimizing (7), ridge (top left) and LASSO (bottom left) coefficient values are simply  $\widehat{G}(\mathbb{1}, \lambda)$ , which generates the curves in Figure 5 by letting  $\lambda$  vary from 0.0006 to 0.6. The resulting solution-paths of the GMS ridge and LASSO procedures show that the proposed method approximates the standard ones obtained by LARS (Efron et al., 2004) very accurately.

We further investigate how the GMS-bootstrap helps to quantify uncertainty in choosing  $\lambda$ . Figure 6 illustrates some benefits of the bootstrapped CV procedure for the LASSO example. The left panel shows a 95% confidence band for the CV errors across  $\lambda$ . As Efron and Tibshirani (1997) noted, the bootstrapped CV improves the performance of prediction error estimation. However, due to heavy computational burden in the standard bootstrap algorithm, applications of the bootstrapped CV have been greatly hindered. The example in Figure 6 shows that the GMS helps overcome this computational difficulty. The center panel depicts the bootstrap distribution of the minimizer  $\lambda$  of the CV errors (the red line is the estimated density function). If the CV error curve is of main interest, one can easily generate it by the GMS using binary weights (corresponding to the chosen and left-out folds) as the input. In the right panel of Figure 6, the CV error curve obtained by the standard CV computation is nearly identical to that by the GMS.

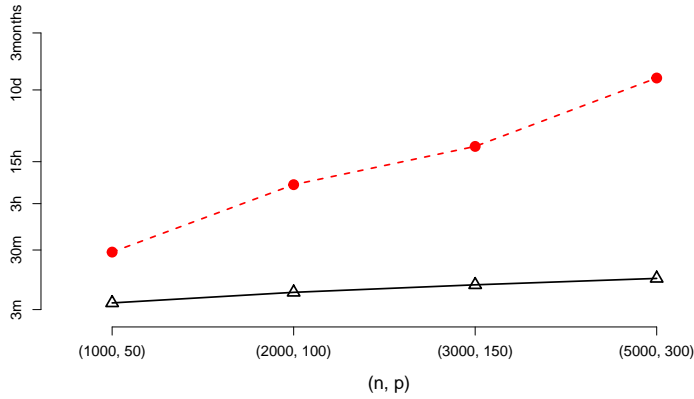


Figure 7: Computation time for the GMS quantile regression (black solid line with triangle marks) and its conventional counterpart (red dashed line with filled-dot marks).

## 5 Quantile Regression Inference at Various Quantile Levels

Quantile regression models, which assume that a certain quantile of the response variable linearly depends on the covariates, have been commonly used for robust regression analysis (Yu et al., 2003; Yu and Moyeed, 2001; Koenker, 2004). More precisely, for a given  $\eta \in (0, 1)$ , the conditional  $\eta$ -th quantile of the response given  $X_i$  is modeled by  $X_i^T \theta$ . The standard loss function for fitting such a model is

$$\ell(\theta; y_i, X_i) = \rho_\eta(y_i - X_i^T \theta), \quad (8)$$

where  $\rho_\eta(u) = (\eta - I(u < 0))u$ . The inference for the regression coefficients in this setting is more challenging than that for parametric regression models, because the sampling distribution of the coefficient estimates often relies on the regression error density function, which needs to be estimated and is a challenging task by itself in high-dimensional settings (Koenker, 1994). In routine applications of quantile regression analyses, bootstrap procedures are popular to use for approximating the sampling distribution of the estimates (Feng et al., 2011; Hahn, 1995; Kocherginsky et al., 2005), which can be computationally demanding. Furthermore, when a practitioner is interested in investigating multiple quantile levels, it is also necessary to repeat the bootstrap procedure multiple times, each at a different quantile level. Such a computational burden is prohibitive when the data size is large.

By using  $\ell(G(\mathbf{w}, \eta); y_i, X_i) = \rho_\eta(y_i - X_i^T G(\mathbf{w}, \eta))$  in (3), we apply the GMS to overcome the computational challenges for the inference of quantile regression models with a GMS loss of

$$\hat{G} = \underset{G}{\operatorname{argmin}} \mathbb{E}_{\mathbf{w}, \eta} \left[ \sum_i^n w_i \rho_\eta(y_i - X_i^\top G(\mathbf{w}, \eta)) \right], \quad (9)$$

where  $\mathbb{E}_{\mathbf{w}, \eta}$  is the expectation operator on  $\mathbf{w}$  and  $\eta$ , assuming that  $\eta$  follows some distribution  $\mathbb{P}_\eta$  whose support is  $(0,1)$  and independent with  $\mathbf{w}$ . A default choice is to add random noises to the candidate set of quantile levels, and let  $\mathbf{w}$  follow the probability law in (6).

To demonstrate the effectiveness of this procedure, we test the method on a simulation setting examined in Feng et al. (2011). The data set is generated from the model  $y_i = X_i^\top \theta_0 + 3^{-1/2}[2 + \{1 + (x_{1i} - 8)^2 + x_{2i}\}/10]\epsilon_i$ ,  $i = 1, \dots, n$ , where  $X_i = (x_{i1}, \dots, x_{ip})^\top$ ,  $n = 500$ ,  $p = 5$ ,  $\theta_0 = \mathbb{1}_5^\top$ , and  $\epsilon_i \sim t_3$ . We let  $x_{2i} = 1$  for  $i \leq 400$  and  $= 0$  for  $i > 400$ , and generate the other covariates independently from the standard log-normal distribution. Figure 8 (b)–(d) compare the 90% confidence bands of several coefficients generated by the GMS with those obtained by the standard bootstrap over quantiles varying from 0.05 and 0.95, showing that the approaches result in nearly identical bands.

To investigate computational efficiency of the GMS for quantile regression, we increase the sample size and the number of predictors in the above simulation model to  $(n, p) = (1000, 50)$ ,  $(2000, 100)$ ,  $(3000, 150)$ , and  $(5000, 300)$ , respectively, and consider quantile levels varying from 0.05 to 0.95 with a skip of 0.05 (total 19 quantile levels). We set the first five coefficients of  $\theta_0$  to be one and the others be zero. Our target is to obtain 5,000 bootstrap samples under each setting. Due to heavy computational burden of the standard bootstrap procedure, we compute only five bootstrap evaluations and report an estimated time from them (e.g., multiplying 1,000 to the time taken for the five evaluations). Figure 8 (a) depicts the computation time required for each procedure. While the GMS can be trained in less than 10 minutes for moderately large data size ( $n = 5000, p = 300$ ), the standard bootstrap requires more than 30 minutes for the smallest data set ( $n = 1000, p = 50$ ) and about 3 months for the case of ( $n = 5000, p = 300$ ).

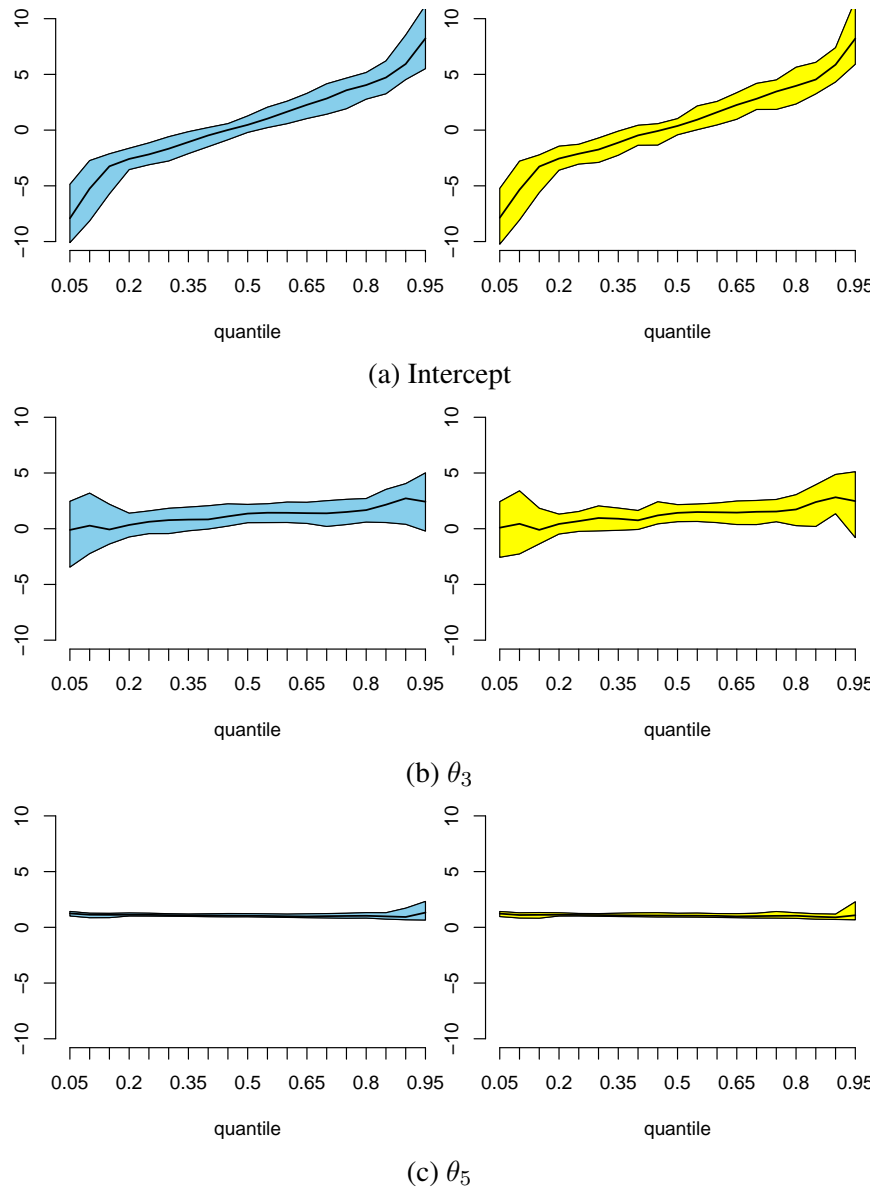


Figure 8: (a): The red dots and black triangles depict the computation times required by the standard bootstrap and the GMS, respectively, in generating 5,000 bootstrap estimators. (b)–(d): Comparisons between the 90% confidence bands obtained from the GMS (blue) and the classical bootstrap (yellow) across quantile levels ranging from 5% to 95%. The `quantreg` R package is used for the conventional.

## 6 Computational Strategies for Training the Generator

### 6.1 Multilayer perceptron

*Neural networks* have been shown effective for approximating functions with complicated structures. Recently, researchers have experimented with various novel ways of using neural networks, such as constructing generators of real-life-like images and creating generative adversarial networks for approximating high-dimensional distributions (Ledig et al., 2017; Wang et al., 2018; Karras et al., 2018; Goodfellow et al., 2014; Arjovsky et al., 2017). The simplest neural network structure is a class of MLPs/FNNs constructed by composing activated linear transformations. For  $k = 1, \dots, K$ , let  $g_k$  denote the feed-forward mapping represented by  $N^{(k)}$  hidden nodes, where  $g_k : \mathbb{R}^{N^{(k)}} \mapsto \mathbb{R}^{N^{(k+1)}}$  is defined as  $g_k(\mathbf{X}) = \sigma(\mathbf{U}^{(k)}\mathbf{X} + \mathbf{b}^{(k)}) \in \mathbb{R}^{N^{(k+1)}}$ , where  $\mathbf{X} \in \mathbb{R}^{N^{(k)}}$  is the input variable of  $g_k$ . Also, this function is characterized by a “weight” parameter and a “bias” parameter: the  $N^{(k+1)} \times N^{(k)}$  weight matrix  $\mathbf{U}^{(k)}$  and the  $N^{(k+1)}$ -dimensional bias vector  $\mathbf{b}^{(k)} = \{b_1^{(k)}, \dots, b_{N^{(k+1)}}^{(k)}\}$ . A  $K$ -layer MLP function  $g : \mathbb{R}^{N^{(1)}} \mapsto \mathbb{R}^D$  can be defined by the composition of these functions as

$$g(\mathbf{X}) = L \circ g_K \circ \dots \circ g_1(\mathbf{X}), \quad (10)$$

where  $L : \mathbb{R}^{N^{(K)}} \mapsto \mathbb{R}^D$  is a linear function that maps the final hidden layer  $g_K \circ \dots \circ g_1(\mathbf{X})$  to the  $D$ -dimensional output space of  $g$ . Commonly used activation functions include the sigmoid function, the hyperbolic tangent function, the Rectified Linear Unit (ReLU) (Nair and Hinton, 2010), the Exponential Linear Unit (Clevert et al., 2015), the Gaussian Error Linear Unit (Hendrycks and Gimpel, 2016), etc. We here employ neural networks with the ReLU activation function  $\sigma(t) = \max\{t, 0\}$  to construct generator  $G$  in (3) in a novel way as characterized by the integrative loss (3) and the weight multiplicative MLP explained below.

### 6.2 Weight multiplicative MLP

Despite its generalizability and practicability, we observe that the simple MLP converges slowly for our GMS applications (as shown in Figure 9). We propose a modification motivated by

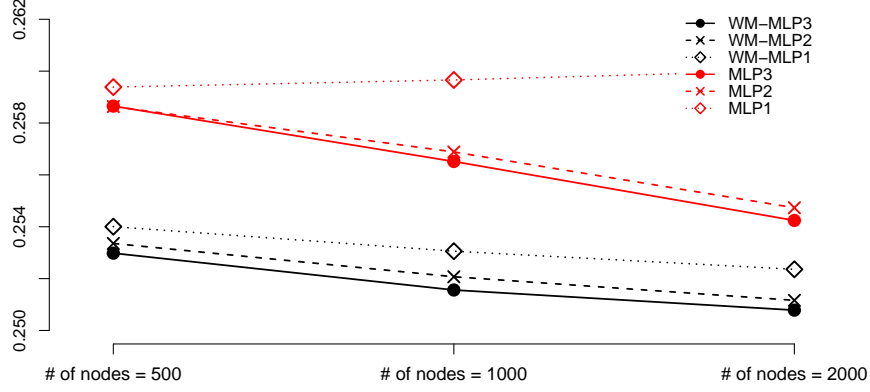


Figure 9: Comparison of the losses obtained by the simple MLP and the WM-MLP with various numbers of hidden layers and nodes. The number noted after "MLP" indicates the number of layers  $K$ .

the Taylor approximation of the first derivative of the weighted loss function. For illustration, let us consider the weighted M-estimation loss  $\sum_{i=1}^n w_i \ell(\theta; y_i)$  and its optimizer  $\hat{\theta}_{\mathbf{w}}$  in (1) for a case of  $p = 1$  (ignoring  $\eta$  and  $\lambda$  for simplicity). Under mild conditions, we assume that  $\sum_{i=1}^n w_i \ell'(\hat{\theta}_{\mathbf{w}}; y_i) = 0$ , where  $\ell'$  is the first derivative of  $\ell$  with respect to  $\theta$ . Then, by using a Taylor approximation of  $\ell'$  at a local region of some arbitrary  $g(\mathbf{w})$ , we obtain that

$$0 = \sum_{i=1}^n w_i \ell'(\hat{\theta}_{\mathbf{w}}; y_i) \approx \sum_{i=1}^n w_i \ell'(g(\mathbf{w}); y_i) + \sum_{i=1}^n w_i \ell''(g(\mathbf{w}); y_i) (\hat{\theta}_{\mathbf{w}} - g(\mathbf{w})),$$

where  $\ell''(\theta, y)$  denotes the second derivative of  $\ell$  with respect to  $\theta$ . Thus, we have

$$\hat{\theta}_{\mathbf{w}} \approx g(\mathbf{w}) - \sum_{i=1}^n \frac{w_i \ell'(g(\mathbf{w}); y_i)}{\sum_{j=1}^n w_j \ell''(g(\mathbf{w}); y_j)} \triangleq g(\mathbf{w}) + \sum_{i=1}^n w_i h_i(\mathbf{w}). \quad (11)$$

Motivated by this approximation, we propose a new neural network structure called the *Weight Multiplicative MLP* (WM-MLP) as the sum of a simple MLP and a weight multiplicative one:

$$G(\mathbf{w}, \lambda, \eta) = \underbrace{L_1 \circ B_K(\mathbf{w}, \lambda, \eta)}_{\text{Simple MLP: } g(\mathbf{w})} + \underbrace{L_2 \circ (\{f \circ B_K(\mathbf{w}, \lambda, \eta)\} \odot \mathbf{w})}_{\text{Weight multiplicative network: } \sum_{i=1}^n w_i h_i(\mathbf{w}, \lambda, \eta)}, \quad (12)$$

where " $\odot$ " indicates an element-wise multiplication operator;  $L_1 : \mathbb{R}^H \mapsto \mathbb{R}^p$  and  $L_2 : \mathbb{R}^n \mapsto \mathbb{R}^p$  are linear functions;  $B_K : \mathbb{R}^{n+1+1} \mapsto \mathbb{R}^H$  and  $f : \mathbb{R}^H \mapsto \mathbb{R}^n$  are simple MLPs with  $K$  hidden

---

**Algorithm 1** A general algorithm to train the GMS.

---

- Set  $\mathbb{P}_{\alpha, \lambda, \eta}$ ,  $S$  (subgroup size),  $M$  (Monte Carlo sample size), and  $T$  (total iterations).
  - Randomly split the full data into  $S$  subgroups, resulting in an index function  $h(\cdot)$  in (6).
  - Initialize the neural net parameter  $\phi^{(0)}$ .
  - Set  $t = 0$ .
  - while** the stop condition is not satisfied or  $t < T$  **do**
    - Independently sample  $M$  values of  $\alpha$ 's,  $\lambda$ 's, and  $\eta$ 's from  $\mathbb{P}_{\alpha, \lambda, \eta}$ .
    - Consider  $L = \frac{1}{M} \sum_{m=1}^M \sum_{i=1}^n \alpha_{h(i)}^{(m)} l(G_{\phi^{(t)}}(\alpha^{(m)}, \lambda^{(m)}, \eta^{(m)}); y_i) / n + \lambda^{(m)} u(G_{\phi^{(t)}}(\alpha^{(m)}, \lambda^{(m)}, \eta^{(m)}))$ , where  $\alpha^{(m)}$  is the  $m$ -th sample of  $M$   $\alpha$ 's.
    - Update  $\phi^{(t+1)}$  by using the gradient of  $L$  via a SGD step.
    - Let  $t = t + 1$ .
  - end while**
- 

layers and one hidden layer, respectively. For a large  $n$ , the subgroup bootstrap in Section 3.1 reduces the dimension of  $\mathbf{w}$  and the network size.

To demonstrate the improvement, we compare the performances of WM-MLP and the simple MLP for various sizes of hidden nodes (500, 1000, 2000) and layers ( $K = 1, 2, 3$ ), for a logistic regression example. The true  $\theta$ 's in the simulations are equi-spaced between  $-0.5$  and  $0.5$  with  $p = 100$  and  $n = 1000$ . We train the generator  $G$  from ten random initializations and report the average loss values after 30,000 iterative updates for each MLP structure. The results are summarized in Figure 9, demonstrating that for all network sizes the proposed WM-MLP outperforms the simple MLP uniformly. In comparison to a large-sized MLP with three hidden layers and 2000 neurons, even a small-scale WM-MLP with a single hidden layer and 500 neurons achieves a lower loss, whereas the simple MLP with one hidden layer performs much poorly. For all examples in the paper, we used the WM-MLP with three hidden layers as a default, and observed that the resulting generator function based on the WM-MLP performed satisfactorily.

### 6.3 Computational strategy in optimization

It is straightforward to optimize the GMS integrative loss (3) because the expectation can be approximated by a few Monte Carlo samples at each iteration. We use a variant of the popular SGD algorithms such as *Adam* (Kingma and Ba, 2014), *AdaGrad* (Duchi et al., 2011), *RMSProp* (Tieleman et al., 2012), etc, to iteratively update the neural net parameters until the algorithm converges. Algorithm 1 summarizes the detailed steps of the GMS. As in (4), this algorithm samples  $M$  values of  $\mathbf{w}$ 's and  $\lambda$ 's to approximate the expectation and updates the neural network



parameters via SGD. It is not uncommon nowadays for a data set to be extremely large, to the point that the full data size surpasses the memory capacity of the computer in use. Data sub-sampling would be advantageous in this setting for training the GMS, which partially updates the weights corresponding to the subsampled data in the same spirit as stochastic optimization (Allen-Zhu et al., 2019).

**Technical details of the optimization.** In all our examples, we use the WM-MLP with three hidden layers and 1,000 hidden neurons in each layer. In `Pytorch`, algorithm Adam is used with a learning rate of 0.0003 and a decay rate of  $t^{-0.3}$  by default. We use full samples in the SGD optimization without mini-batches because the data sizes of the examples we considered are manageable. However, when the data size is massive, minibatch subsampling would be necessary.

**Choosing distributions for  $\mathbf{w}$ ,  $\lambda$ , and  $\eta$ .** For bootstrap procedures, the distribution of bootstrap weights  $\mathbf{w}$  (or  $\alpha$ ) can be easily chosen depending on the practitioner’s interest; e.g.,  $\mathbf{w} \sim \text{Multinomial}(n, \mathbb{1}_n/n)$  or  $\mathbf{w} \sim n \times \text{Dirichlet}(n, \mathbb{1}_n)$ . When  $n$  is excessively large, the dimension of  $\mathbf{w}$  can be reduced by the subgroup bootstrapping method in Section 3.1. As a general rule, when  $n > 500$ , we recommend considering subgrouping. While our theoretical evidence suggests that  $S \succ n^{1/2}$  is optimal (see Section A.1 in Supplementary Materials), empirically setting  $S$  to a few hundreds performs well in all situations shown in this paper. By default,  $S = 100$  was used. Choosing the training distributions for  $\lambda$  and  $\eta$  is more arbitrary because usually we have no reference distributions for  $\lambda$  and  $\eta$  unlike the case of  $\mathbf{w}$ . We may first set candidate sets for  $\lambda$  and  $\eta$  in advance (which can be large in size) and then add some random noises to form mixture distributions. For example, we can generate  $\lambda = \exp\{\log \lambda' + \epsilon\}$ , where  $\lambda'$  is randomly selected from the candidate set and  $\epsilon \sim N(0, \delta)$  with  $\delta = 0.2^2$  as default. For the quantile regression example in Section 5, we generate  $\eta = \eta' + N(0, 0.03^2)$  with  $\eta'$  randomly selected from a pre-determined candidate set, and then truncated to be in  $(0.001, 0.999)$ .

**Training stopping criteria.** In order to judge the convergence in training the generator function, we first set the maximum number of epochs depending on computational resources at hands

(our default is 20,000 epochs). In addition to this stopping criterion, we also consider an *early stopping rule* that has been commonly used in training general neural networks (Heckel and Yilmaz, 2021; Li et al., 2020; Prechelt, 1998) to determine when we stop the optimization algorithm before reaching the maximum number of epochs. Intuitively, we stop the algorithm when the updates do not further reduce the loss value. More specifically, for each epoch  $t$ , we evaluate the averaged loss value  $L^t$  on epoch  $t$  and compare it with those of the previous epochs  $\{L^{t-\ell}, \ell = 1, 2, \dots, k\}$  for some lags. We terminate the SGD algorithm if  $L^t$  is within  $\epsilon$  of a quantile (such as the median) of the previous losses. We recommend to monitor the change of loss values in the previous  $k=100$  epochs, and use the 25th percentile with  $\epsilon = 0.01$ .

## 7 Conclusion

We propose the GMS as a general computational framework to accelerate repeated calculations for (penalized) weighted M-estimations. The GMS was shown effective for a variety of statistical inference procedures, including bootstrap methods and cross-validations for general M-estimators. We apply the GMS to a variety of models, including LASSO, logistic regression, quantile regression, etc. The GMS performs well in all of the situations we investigated, and the weighted M-estimators generated by the GMS are sufficiently accurate and comparable to the much more computationally expensive traditional solutions for all inference purposes. By lowering the computational barrier associated with repetitious data-splitting or data-sampling processes such as (bootstrapped) CVs and iterated bootstrap, the GMS opens up a new perspective on modern statistics. To date, these approaches have been less noticed and rarely practiced by the statistical community not because they are less valuable, but because their computation cost is prohibitively high. We expect that the GMS will prove to be an effective tool for augmenting the power of statistical models in the era of big data.

## References

- Allen-Zhu, Z., Y. Li, and Z. Song (2019). A convergence theory for deep learning via overparameterization. In *International Conference on Machine Learning*, pp. 242–252. PMLR.
- Arjovsky, M., S. Chintala, and L. Bottou (2017). Wasserstein generative adversarial networks. In *International Conference on Machine Learning*, pp. 214–223.
- Barbe, P. and P. Bertail (2012). *The weighted bootstrap*, Volume 98. Springer Science & Business Media.
- Chatterjee, S., A. Bose, et al. (2005). Generalized bootstrap for estimating equations. *The Annals of Statistics* 33(1), 414–436.
- Cheng, G. and J. Z. Huang (2010). Bootstrap consistency for general semiparametric m-estimation. *The Annals of Statistics* 38(5), 2884–2915.
- Clevert, D.-A., T. Unterthiner, and S. Hochreiter (2015). Fast and accurate deep network learning by exponential linear units (elus). *arXiv preprint arXiv:1511.07289*.
- Cybenko, G. (1989). Approximation by superpositions of a sigmoidal function. *Mathematics of control, signals and systems* 2(4), 303–314.
- Diciccio, T. and B. Efron (1992). More accurate confidence intervals in exponential families. *Biometrika* 79(2), 231–245.
- Duchi, J., E. Hazan, and Y. Singer (2011). Adaptive subgradient methods for online learning and stochastic optimization. *Journal of machine learning research* 12(7).
- Efron, B. (1979). Bootstrap methods: Another look at the jackknife. *The Annals of Statistics* 7(1), 1–26.
- Efron, B. (1987). Better bootstrap confidence intervals. *Journal of the American statistical Association* 82(397), 171–185.
- Efron, B., T. Hastie, I. Johnstone, and R. Tibshirani (2004). Least angle regression. *The Annals of statistics* 32(2), 407–499.

- Efron, B. and R. Tibshirani (1997). Improvements on cross-validation: the 632+ bootstrap method. *Journal of the American Statistical Association* 92(438), 548–560.
- Efron, B. and R. J. Tibshirani (1994). *An introduction to the bootstrap*. CRC press.
- Feng, X., X. He, and J. Hu (2011). Wild bootstrap for quantile regression. *Biometrika* 98(4), 995–999.
- Geer, S. A., S. van de Geer, and D. Williams (2000). *Empirical Processes in M-estimation*, Volume 6. Cambridge university press.
- Goodfellow, I., J. Pouget-Abadie, M. Mirza, B. Xu, D. Warde-Farley, S. Ozair, A. Courville, and Y. Bengio (2014). Generative adversarial nets. In *Advances in neural information processing systems*, pp. 2672–2680.
- Hahn, J. (1995). Bootstrapping quantile regression estimators. *Econometric Theory* 11(1), 105–121.
- Hall, P. (1986). On the bootstrap and confidence intervals. *The Annals of Statistics*, 1431–1452.
- Hall, P. (1988). Theoretical comparison of bootstrap confidence intervals. *The Annals of Statistics*, 927–953.
- Hall, P. (1992). On bootstrap confidence intervals in nonparametric regression. *The Annals of Statistics*, 695–711.
- Hall, P. (2013). *The bootstrap and Edgeworth expansion*. Springer Science & Business Media.
- Hall, P. and M. A. Martin (1988). On bootstrap resampling and iteration. *Biometrika* 75(4), 661–671.
- Härdle, W., J. Horowitz, and J.-P. Kreiss (2003). Bootstrap methods for time series. *International Statistical Review* 71(2), 435–459.
- Heckel, R. and F. F. Yilmaz (2021). Early stopping in deep networks: Double descent and how to eliminate it. In *International Conference on Learning Representations*.

- Hendrycks, D. and K. Gimpel (2016). Gaussian error linear units (gelus). *arXiv preprint arXiv:1606.08415*.
- Hoerl, A. E. and R. W. Kennard (1970). Ridge regression: Biased estimation for nonorthogonal problems. *Technometrics* 12(1), 55–67.
- Huber, P. J. (1992). Robust estimation of a location parameter. In *Breakthroughs in statistics*, pp. 492–518. Springer.
- Karras, T., T. Aila, S. Laine, and J. Lehtinen (2018). Progressive growing of gans for improved quality, stability, and variation. In *International Conference on Learning Representations*.
- Kingma, D. P. and J. Ba (2014). Adam: A method for stochastic optimization. *arXiv preprint arXiv:1412.6980*.
- Kleiner, A., A. Talwalkar, P. Sarkar, and M. I. Jordan (2014). A scalable bootstrap for massive data. *Journal of the Royal Statistical Society: Series B (Statistical Methodology)* 76(4), 795–816.
- Kocherginsky, M., X. He, and Y. Mu (2005). Practical confidence intervals for regression quantiles. *Journal of Computational and Graphical Statistics* 14(1), 41–55.
- Koenker, R. (1994). Confidence intervals for regression quantiles. In *Asymptotic statistics*, pp. 349–359. Springer.
- Koenker, R. (2004). Quantile regression for longitudinal data. *Journal of Multivariate Analysis* 91(1), 74–89.
- Kosorok, M. R. (2008). M-estimators. *Introduction to Empirical Processes and Semiparametric Inference*, 263–282.
- Lahiri, S. N. (1999). Theoretical comparisons of block bootstrap methods. *Annals of Statistics*, 386–404.
- Ledig, C., L. Theis, F. Huszár, J. Caballero, A. Cunningham, A. Acosta, A. Aitken, A. Tejani, J. Totz, Z. Wang, et al. (2017). Photo-realistic single image super-resolution using a generative

- adversarial network. In *Proceedings of the IEEE conference on computer vision and pattern recognition*, pp. 4681–4690.
- Lee, S. M. and G. A. Young (1995). Asymptotic iterated bootstrap confidence intervals. *The Annals of Statistics*, 1301–1330.
- Lee, S. M. and G. A. Young (1999). The effect of monte carlo approximation on coverage error of double-bootstrap confidence intervals. *Journal of the Royal Statistical Society: Series B (Statistical Methodology)* 61(2), 353–366.
- Li, M., M. Soltanolkotabi, and S. Oymak (2020). Gradient descent with early stopping is provably robust to label noise for overparameterized neural networks. In *International Conference on Artificial Intelligence and Statistics*, pp. 4313–4324. PMLR.
- Lu, Z., H. Pu, F. Wang, Z. Hu, and L. Wang (2017). The expressive power of neural networks: A view from the width. In *Proceedings of the 31st International Conference on Neural Information Processing Systems*, pp. 6232–6240.
- Martin, M. A. (1992). On the double bootstrap. In *Computing science and statistics*, pp. 73–78. Springer.
- McCarthy, D., K. Zhang, L. D. Brown, R. Berk, A. Buja, E. I. George, and L. Zhao (2018). Calibrated percentile double bootstrap for robust linear regression inference. *Statistica Sinica* 28(4), 2565–2589.
- Nair, V. and G. E. Hinton (2010). Rectified linear units improve restricted boltzmann machines. In *Proceedings of the 27th International Conference on International Conference on Machine Learning*, pp. 807–814.
- Newton, M. A. and A. E. Raftery (1994). Approximate Bayesian inference with the weighted likelihood bootstrap. *Journal of the Royal Statistical Society: Series B (Methodological)* 56(1), 3–26.
- Præstgaard, J. and J. A. Wellner (1993). Exchangeably weighted bootstraps of the general empirical process. *The Annals of Probability*, 2053–2086.

- Prechelt, L. (1998). Early stopping-but when? In *Neural Networks: Tricks of the trade*, pp. 55–69. Springer.
- Rubin, D. B. (1981). The Bayesian bootstrap. *The Annals of Statistics* 9(1), 130434.
- Rumelhart, D. E., G. E. Hinton, and R. J. Williams (1986). Learning representations by back-propagating errors. *nature* 323(6088), 533–536.
- Tibshirani, R. (1996). Regression shrinkage and selection via the lasso. *J. R. Statist. Soc. B*, 267–288.
- Tieleman, T., G. Hinton, et al. (2012). Lecture 6.5-rmsprop: Divide the gradient by a running average of its recent magnitude. *COURSEERA: Neural networks for machine learning* 4(2), 26–31.
- Wang, T.-C., M.-Y. Liu, J.-Y. Zhu, A. Tao, J. Kautz, and B. Catanzaro (2018). High-resolution image synthesis and semantic manipulation with conditional gans. In *Proceedings of the IEEE conference on computer vision and pattern recognition*, pp. 8798–8807.
- Xu, L., C. Gotwalt, Y. Hong, C. B. King, and W. Q. Meeker (2020). Applications of the fractional-random-weight bootstrap. *The American Statistician*, 1–21.
- Yu, K., Z. Lu, and J. Stander (2003). Quantile regression: applications and current research areas. *Journal of the Royal Statistical Society: Series D (The Statistician)* 52(3), 331–350.
- Yu, K. and R. A. Moyeed (2001). Bayesian quantile regression. *Statistics & Probability Letters* 54(4), 437–447.

# Supplementary Materials for “Generative Multi-purpose Sampler for Weighted M-estimation”

## A Theoretical Results

### A.1 Theoretical Justification of Subgroup Bootstrap

While subgrouping was shown empirically to approximate the target bootstrap distribution well, its theoretical consistency is not immediately apparent. Here we employ the theoretical tools described in Cheng and Huang (2010) to examine theoretical aspects of subgrouping bootstrap procedures for the general M-estimation. Let  $Y_1, Y_2, \dots$  be a sequence of iid random variables (with their observed values  $y_1, y_2, \dots$ ) from the probability distribution  $\mathbb{P}_0$  with the true parameter  $\theta_0$ , and the resulting expectation is denoted by  $\mathbb{E}_0$ . The probability distribution of  $\mathbf{w}$  and its expectation are denoted by  $\mathbb{P}_{\mathbf{w}}$  and  $\mathbb{E}_{\mathbf{w}}$ , respectively. The empirical measure of the observations and the expectation with respect to it are denoted by  $\hat{P}_n$  and  $\hat{\mathbb{E}}_n$ , respectively. We also define a weighted bootstrap empirical measure  $\hat{\mathbb{P}}_{\mathbf{w},n} = \sum_{i=1}^n w_i \delta_{y_i} / n$ , where  $\delta_t$  is a point measure at  $t$ , and the expectation with respect to it is denoted by  $\hat{\mathbb{E}}_{\mathbf{w},n}$ . We let  $\ell'$  and  $\ell''$  denote the first and second order derivatives of  $\ell(\theta; Y)$  with respect to  $\theta$ , respectively. The original M-estimator, which corresponds to the solution of (1) with  $\mathbf{w} = \mathbf{1}$ , is denoted by  $\hat{\theta}$ . The big “ $O_{\mathbb{P}_0}$ ” and small “ $o_{\mathbb{P}_0}$ ” are based on probability distribution  $\mathbb{P}_0$ . We then consider some regularity conditions below:

- (A1) There exists  $\epsilon > 0$  such that  $\mathbb{E}_0[\ell'(\theta) - \ell'(\theta_0)] = \mathbb{E}_0[\ell''(\theta_0)(\theta - \theta_0)] + O(\|\theta - \theta_0\|^2)$ , if  $\|\theta - \theta_0\| < \epsilon$  for large enough  $n$ .
- (A2) Suppose that  $\mathbb{E}_0[\ell'(\theta_0)] = 0$ ,  $\hat{\mathbb{E}}_n[\ell'(\hat{\theta})] = o_{\mathbb{P}_0}(\sqrt{n})$ , and  $\hat{\mathbb{E}}_{\mathbf{w},n}[\ell'(\hat{\theta}_{\mathbf{w}})] = o_{\mathbb{P}_0}(\sqrt{n})$ . Also, assume that the optimizers  $\hat{\theta}$  and  $\hat{\theta}_{\mathbf{w}}$  are unique over  $\mathcal{W}$ .
- (A3) There exists  $\delta > 0$  such that  $\hat{\mathbb{E}}_n[\ell'(\theta) - \ell'(\theta_0)] - \mathbb{E}_0[\ell'(\theta) - \ell'(\theta_0)] = O_{\mathbb{P}_0}(\sqrt{n}\|\theta - \theta_0\|)$ , if  $\|\theta - \theta_0\| < \delta$ .
- (A4) The variance of  $\ell'(\theta_0)$  and  $\mathbb{E}_0[\ell''(\theta_0)]$  are both non-singular.

These or similar mild regularity conditions are often required for showing asymptotic con-



sistency of M-estimators as in (Kosorok, 2008; Geer et al., 2000). Condition **(A1)** assures that the derivative of the loss is smooth enough to be linearly approximated around a local region at the true parameter. Condition **(A2)** assumes the uniqueness of the minimizers, and is general enough to deal with the case that the estimator and its bootstrap version are not exact minimizers, but “nearly-minimizing” the target losses. Condition **(A3)** is called the *stochastic equi-continuity* (Cheng and Huang, 2010) and guarantees that the discrepancy between the empirical and true derivatives of the loss around the true parameter is of order  $\sqrt{n}$ . Condition **(A4)** ensures that the considered estimator asymptotically attains a non-singular variance.

Under the same regularity conditions as described in Section 3.1, Cheng and Huang (2010) imposed the following set of additional conditions on the weight distribution in order to guarantee the bootstrap consistency:

W1. The distribution of the weight vector  $\mathbf{w} = (w_1, \dots, w_n)$  is exchangeable for all  $n = 1, 2, \dots$ .

W2.  $\forall i, w_i \geq 0$ , and  $\sum_{i=1}^n w_i = n$ .

W3.  $\exists C < \infty$ , such that  $\limsup_{n \rightarrow \infty} \|w_1\|_{2,1} \leq C$ , where  $\|w_1\|_{2,1} = \int_0^\infty \sqrt{P_{\mathbf{w}}(w_1 \geq u)} du$ .

W4.  $\lim_{\lambda \rightarrow \infty} \limsup_{n \rightarrow \infty} \sup_{t \geq \lambda} t^2 P_{\mathbf{w}}(w_1 > t) = 0$ .

W5.  $\sum_{i=1}^n (w_i - 1)^2 / n \xrightarrow{P} c^2$  with respect to  $\mathbb{P}_{\mathbf{w}}$  for some constant  $c > 0$ .

**Theorem A.1.** (Cheng and Huang, 2010). *Assume that **(A1)** – **(A4)** hold, and the subgroups are randomly assigned. Consider a random weight bootstrap with  $\mathbf{w} \sim \mathbb{P}_{\mathbf{w}}$  that satisfy W1–W5. Then, the resulting subgroup bootstrap is consistent; i.e.,*

$$\sup_{x \in \mathbb{R}^p} \left| \mathbb{P}_{\mathbf{w}|D_n}(\sqrt{n}(\hat{\theta}_{\mathbf{w}} - \hat{\theta}) \leq x) - \mathbb{P}_0(\sqrt{n}(\hat{\theta} - \theta_0) \leq x) \right| \rightarrow 0,$$

in  $\mathbb{P}_0$ -probability as  $n$  tends to  $\infty$ .

Thus, it is sufficient to show that the subgroup bootstrap satisfies W1–W5. First, condition W2 is trivially true. Since the marginal distribution of  $w_1$  follows  $\text{Beta}(1, S - 1)$ , conditions W3 and W4 are satisfied. For W5, because  $\mathbb{E}\{(w_1 - 1)^2\} = 1 - 2/(S + 1)$ , the subgroup weights satisfy W5.

Now it is sufficient to show that the exchangeability holds as in W1 to show the consistency of the bootstrap. However, the members of each subgroup is fixed in advance, which breaks the exchangeability condition among the bootstrap weights. Instead, we show that the subgroup bootstrap with fixed subgroups is consistent with an exchangeable subgroup bootstrap with a random subgrouping.

As an opponent of the proposed fixed subgrouped weight  $\mathbf{w}_S = \{w_{S,1}, \dots, w_{S,n}\}$  with deterministic subgroup indexes  $\{I_1, \dots, I_S\}$ , we first consider a fully randomized subgroup bootstrap weight  $\tilde{\mathbf{w}}_S = \{\tilde{w}_{S,1}, \dots, \tilde{w}_{S,n}\}$  that assumes the subgroups are also randomly assigned for every bootstrap evaluation. Like the subgroup weights, its weights are also generated from  $\{\tilde{\alpha}_{S,1}, \dots, \tilde{\alpha}_{S,S}\} \sim S \times \text{Dirichlet}(S, \mathbb{1}_S)$ . As a result, it is trivial that the distribution of  $\tilde{\mathbf{w}}_S$  is exchangeable, as well as satisfying W2–W5. Then, it follows that for any bounded and continuous function  $f$ ,

$$\begin{aligned}
& \text{Var} \left( \frac{1}{\sqrt{n}} \sum_{i=1}^n (w_{S,i} - 1) f(y_i) \mid \mathbf{y} \right) = \mathbb{E} \left( \left\{ \frac{1}{\sqrt{n}} \sum_{i=1}^n (w_{S,i} - \tilde{w}_{S,i} + \tilde{w}_{S,i} - 1) f(y_i) \right\}^2 \mid \mathbf{y} \right) \\
& = \mathbb{E} \left( \left\{ \frac{1}{\sqrt{n}} \sum_{i=1}^n (w_{S,i} - \tilde{w}_{S,i}) f(y_i) \right\}^2 \mid \mathbf{y} \right) \dots \dots \dots \text{(A1)} \\
& + 2\mathbb{E} \left( \left\{ \frac{1}{\sqrt{n}} \sum_{i=1}^n (w_{S,i} - \tilde{w}_{S,i}) f(y_i) \right\} \left\{ \frac{1}{\sqrt{n}} \sum_{i=1}^n (\tilde{w}_{S,i} - 1) f(y_i) \right\} \mid \mathbf{y} \right) \dots \dots \text{(A2)} \\
& + \text{Var} \left( \frac{1}{\sqrt{n}} \sum_{i=1}^n (\tilde{w}_{S,i} - 1) f(y_i) \mid \mathbf{y} \right) \dots \dots \dots \text{(A3)}.
\end{aligned}$$

Because the fully randomized subgroup bootstrap is consistent, the corresponding variance part (A3) in the above equation should be non-zero. As a result, it is sufficient to show that the other term (A1) + (A2) converges to zero in probability with respect to the probability measure  $\mathbb{P}_{\mathbf{y}}$ .

After a simple arithmetic, it follows that

$$\begin{aligned}
& \text{(A1) + (A2)} \\
&= \frac{1}{n} \mathbb{E} \left( \left\{ \sum_{i=1}^n w_{S,i} f(y_i) \right\}^2 - \left\{ \sum_{i=1}^n \tilde{w}_{S,i} f(y_i) \right\}^2 \mid \mathbf{y} \right) \\
&= \frac{1}{n} \mathbb{E} \left( \left\{ \sum_{s=1}^S \alpha_{S,s} \sum_{i \in I_s} f(y_i) \right\}^2 - \left\{ \sum_{s=1}^S \tilde{\alpha}_{S,s} \sum_{i \in \tilde{I}_s} f(y_i) \right\}^2 \mid \mathbf{y} \right).
\end{aligned}$$

Because  $Var(\alpha_{S,1}) = \frac{S-1}{(S+1)}$  and  $Cov(\alpha_{S,1}, \alpha_{S,2}) = -\frac{1}{(S+1)}$ , the above equation follows that

$$\begin{aligned}
& \text{(A1)+(A2)} \\
&= \frac{S-1}{n(S+1)} \sum_{s=1}^S \left[ \left\{ \sum_{i \in I_s} f(y_i) \right\}^2 - \mathbb{E}_{\tilde{I}} \left( \left\{ \sum_{i \in \tilde{I}_s} f(y_i) \right\}^2 \mid \mathbf{y} \right) \right] \dots \dots \text{(B1)} \\
&+ \frac{1}{n(S+1)} \sum_{s \neq k} \left[ \left\{ \sum_{i \in I_s} f(y_i) \right\} \left\{ \sum_{i \in I_k} f(y_i) \right\} - \mathbb{E}_{\tilde{I}} \left( \left\{ \sum_{i \in \tilde{I}_s} f(y_i) \right\} \left\{ \sum_{i \in \tilde{I}_k} f(y_i) \right\} \mid \mathbf{y} \right) \right].
\end{aligned}$$

We show that the variance of (B1) converges to zero as  $n$  grows. Then, by using similar steps, we can show that the rest part converges to zero as well. Because  $\sum_{s=1}^S \sum_{i \in I_s} f(y_i)^2 = \sum_{i=1}^n f(y_i)^2$  for any exclusive subgroups  $\{I_1, \dots, I_S\}$ , it follows that

$$\begin{aligned}
& \sum_{s=1}^S \left\{ \sum_{i \in I_s} f(y_i) \right\}^2 - \sum_{s=1}^S \mathbb{E}_{\tilde{I}} \left( \left\{ \sum_{i \in \tilde{I}_s} f(y_i) \right\}^2 \mid \mathbf{y} \right) \\
&= \sum_{s=1}^S \sum_{\substack{i,l \in I_s \\ i \neq l}} f(y_i) f(y_l) - \sum_{s=1}^S \mathbb{E}_{\tilde{I}} \left( \sum_{\substack{i,l \in \tilde{I}_s \\ i \neq l}} f(y_i) f(y_l) \mid \mathbf{y} \right).
\end{aligned}$$

Therefore, it follows that

$$\begin{aligned}
\text{Var}\{(\mathbf{B1})\} &= \text{Var} \left[ \frac{S-1}{n(S+1)} \sum_{s=1}^S \left\{ \sum_{\substack{i,l \in I_s \\ i \neq l}} f(y_i)f(y_l) - \mathbb{E}_{\tilde{I}} \left( \sum_{\substack{i,l \in \tilde{I}_s \\ i \neq l}} f(y_i)f(y_l) \mid \mathbf{y} \right) \right\} \right] \\
&\leq 2\text{Var} \left[ \frac{S-1}{n(S+1)} \sum_{s=1}^S \sum_{\substack{i,l \in I_s \\ i \neq l}} f(y_i)f(y_l) \right] \\
&= \frac{2(S-1)^2}{n^2(S+1)^2} \sum_{s=1}^S \text{Var} \left[ \sum_{\substack{i,l \in I_s \\ i \neq l}} f(y_i)f(y_l) \right] \\
&= \frac{2S(S-1)^2}{n^2(S+1)^2} \left[ 4(n/S)(n/S-1)\text{Var}\{f(y_1)f(y_2)\} \right. \\
&\quad \left. + 8(n/S)(n/S-1)(n/S-2)\text{Cov}\{f(y_1)f(y_2), f(y_1)f(y_3)\} \right]
\end{aligned}$$

Then, the variance term is  $O(S^{-1})$  and the covariance term is at a rate of  $O(n/S^2)$ . Therefore, the variance of (B1) converges to zero when  $S \succ n^{1/2}$ .  $\square$

## B Details of Double Bootstrap Procedures

We first introduce notation here. Let  $F_0$  and  $\widehat{F}_n$  denote the true distribution function and the empirical distribution of the observed data set, respectively. The bootstrapped version, which is resulted from random sampling the observations with replacement, of  $\widehat{F}_n$  is denoted by  $\widehat{F}_n^*$ . In the same sense, the distribution of double bootstrapped observations, which is a bootstrapped version of  $\widehat{F}_n^*$ , is denoted by  $\widehat{F}_n^{**}$ . We denote the single-bootstrap and double bootstrap estimators resulted from  $\widehat{F}_n^*$  and  $\widehat{F}_n^{**}$  by  $\hat{\theta}^*$  and  $\hat{\theta}^{**}$ , respectively. We let the expectation operators  $\mathbb{E}_0$  and  $\widehat{\mathbb{E}}_n$  be with respect to  $F_0$  and  $\widehat{F}_n$ , respectively.

It is well-known that percentile (or bootstrap-t) CI via a single bootstrap procedure is not calibrated well in a sense that the resulting bootstrapped coverage is not matched to the nominal coverage, and the CI based on these procedures are unnecessarily wide (Efron and Tibshirani, 1994). For a one-sided CI with 95% nominal coverage, the basic idea of these bootstrap is on the

following approximation:

$$\mathbb{P}(T^* > t_\alpha^* \mid \widehat{F}_n) \approx \mathbb{P}_0(T > t_\alpha \mid F_0) = 1 - \alpha,$$

where *i*)  $T = \hat{\theta} - \theta_0$  for the percentile procedure; *ii*)  $T = (\hat{\theta} - \theta_0)/s$ , where  $s$  is the standard error (when unknown, we set  $s = 1$ ), for the studentized procedure, and  $t_\alpha$  is the  $\alpha$  quantile of the distribution of  $T$ . Also,  $T^*$  and  $t_\alpha^*$  are bootstrapped versions of  $T$  and  $t_\alpha$ , respectively. Despite their simple and bootstrap-like intuition, the problem is that the bootstrapped probability  $\mathbb{P}(T^* > t_\alpha^* \mid \widehat{F}_n)$  can be significantly deviated from the target coverage  $1 - \alpha$  in finite samples.

To relieve this problem, Hall and Martin (1988) considered a double bootstrap to calibrate the coverage error for the percentile procedure. This correction searches for a valid quantile level  $\widehat{\alpha}$  in a way that the resulting bootstrap coverage probability approximates  $1 - \alpha$ ; i.e.,  $\mathbb{P}(T^* > t_{\widehat{\alpha}}^* \mid \widehat{F}_n) \approx 1 - \alpha$ . We can approximate such  $\widehat{\alpha}$  by using a double bootstrap, and a bootstrap version of  $\mathbb{P}(T^* > t_\alpha^* \mid \widehat{F}_n)$  can be evaluated via a double-bootstrapped probability  $\mathbb{P}(T^{**} > t_\alpha^{**} \mid \widehat{F}_n^*)$ , where  $T^{**}$  and  $t_\alpha^{**}$  are a double-bootstrapped counterpart of  $T^*$  and  $t_\alpha^*$ . The solution  $\widehat{\alpha}$  can be evaluated by a Monte Carlo approximation as the following steps:

1. Evaluate  $T_b^* = \hat{\theta}_b^* - \hat{\theta}$  and  $T_{bc}^{**} = \hat{\theta}_{bc}^{**} - \hat{\theta}_b^*$  for  $b = 1, \dots, B$  and  $c = 1, \dots, C$ .
2. Construct  $u_b^* = \frac{1}{C} \sum_{c=1}^C \mathbf{1}(T_{bc}^{**} > T_b^*)$  for  $b = 1, \dots, B$ .
3. Set  $\widehat{\alpha} = u_{(B(1-\alpha))}^*$ , where  $u_{(h)}^*$  is the  $h$ -th smallest ordered value of  $\{u_1^*, \dots, u_B^*\}$ .

Then, the calibrated CI can be constructed by  $(-\infty, \hat{\theta} + t_{\widehat{\alpha}}^*)$  for the percentile procedure.

The other approach of double bootstraps is to estimate the standard error of  $\hat{\theta}_b^* - \hat{\theta}$  for the studentized procedure (Hall, 1988). The explicit form of the bootstrap standard error  $\hat{s}_b^*$  of  $\hat{\theta}_b^*$  is frequently unknown, and the second level bootstrap of the  $b$ -th bootstrap data set can be used to evaluate the standard deviation of  $\hat{\theta}_b^*$ ; i.e.,  $\hat{s}_b^* \approx \sqrt{\sum_{c=1}^C (T_{bc}^{**} - \bar{T}_b^*)^2 / (C - 1)}$ , where  $\bar{T}_b^* = \sum_{c=1}^C T_{bc}^{**} / C$ . Then, the resulting one-sided CI with 95% level is  $(-\infty, \hat{\theta} + \tilde{t}_{95\%}^* \hat{s}_b^*)$ , where  $\tilde{t}_\beta^*$  is the  $\beta$ -quantile of  $\{(\hat{\theta}_b^* - \hat{\theta}) / \hat{s}_b^*\}_{b=1, \dots, B}$ , and  $\hat{s}$  is the estimated standard error of  $\hat{\theta}$  from the single bootstrap distribution. By following a similar way, one can construct a two-sided confidence interval by changing lower and upper levels of quantile values.

## C Algorithm for CV generator training

---

**Algorithm 2** A subgroup weight distribution for (bootstrapped)  $K$ -fold CV.

---

**Presetting:**

- Set a candidate set of the tuning parameter  $\{\lambda_1, \dots, \lambda_L\}$ .
- Randomly subgroup the data points into  $S$  blocks  $\{I_1, \dots, I_S\}$  as demonstrated in Section 3.1, and fix them. For simplicity, assume  $\lfloor S/K \rfloor$  to be an integer. Subgroup  $\{I_1, \dots, I_S\}$  into  $K$  folds, say  $\{I_1^*, \dots, I_K^*\}$ , where  $I_k^* = \{I_{(k-1)S/K+1}, \dots, I_{kS/K}\}$  for  $k = 1, \dots, K$  (each fold contains  $S/K$  blocks).

**Sampling:**

- Randomly select one  $k'$  from  $\{1, \dots, K\}$ , and set  $w_i = 0$  for  $i \in I_{k'}^*$ , and the other weights are set to be

$$\{w_i\}_{i \notin I_{k'}^*} \begin{cases} = 1 \text{ for an only CV,} \\ \sim (S - S/K) \times \text{Dirichlet}(S - S/K, \mathbb{1}_{S-S/K}) \\ \text{or Multinomial}(S - S/K, \mathbb{1}_{S-S/K}/(S - S/K)) \text{ for a bootstrapped CV.} \end{cases}$$

---

### C.1 Specifications of Computing System

For the GMS and GBS applications, we used a GPU computing based on `2×RTX2080ti` with 11GB RAM (a parallel GPU computing was not employed, but only a single GPU was used for each setting). For the conventional procedures, the computations were run under a workstation with a CPU of `Threadripper 2990WX` 64 threads with 128GB RAM.